Synthesis and Characterization of Organic and Inorganic Compounds with Biological
Applications

By

Alexander N. Wein

Advisor: Frank E. McDonald

Department of Chemistry

_____
Frank E. McDonald
Advisor

_____
Jack F. Eichler
Committee Member

_____
Leah A. Roesch
Committee Member

_____
April 16, 2010

Synthesis and Characterization of Organic and Inorganic Compounds with Biological
Applications

By

Alexander N. Wein

Advisor: Frank E. McDonald

An abstract of
A thesis submitted to the Faculty of Emory College of Arts and Sciences
of Emory University in partial fulfillment
of the requirements of the degree of
Bachelor of Sciences with Honors

Department of Chemistry

2010

Abstract

Synthesis and Characterization of Organic and Inorganic Compounds with Biological

Applications

By Alexander N. Wein

Progress towards the synthesis of two families of anti-cancer drugs is reported. Gold(III) complexes were made with bidentate amine ligands and tested for DNA binding, thioredoxin reductase inhibition, stability against biological reductants, and cytotoxicity. The results suggest that contrary to current opinion, the cytotoxicity of these types of complexes is not solely due to thioredoxin reductase inhibition and appears to occur via several different processes.

A synthetic route to novel sphingolipids is also reported. These are made by a three part convergent synthesis that allows for control of the stereochemistry of the hydrophilic head. From one highly unsaturated sphingolipid it is possible to selectively reduce and oxidize the molecule to several different compounds allowing for an extended family of conformationally constrained compounds to be made via a subsequent divergent synthesis.

Also reported are a new synthesis of 4-trimethylsilyl-2-butyn-1-ol and a study of the ^{19}F NMR and solid state characteristics of fluorinated copper(II) carboxylates.

Synthesis and Characterization of Organic and Inorganic Compounds with Biological
Applications

By

Alexander N. Wein

Advisor: Frank E. McDonald

A thesis submitted to the Faculty of Emory College of Arts and Sciences
of Emory University in partial fulfillment
of the requirements of the degree of
Bachelor of Sciences with Honors

Department of Chemistry

2010

Acknowledgements

I would like to thank the Oxford College Department of Chemistry and the Oxford College Research Scholars Program, which is supported by the Office of the Academic Dean, the Howard Hughes Medical Institute (grant 52005873), and the Emory SIRE program for providing funding towards this research. I also acknowledge the use of shared instrumentation provided by the NSF and NIH.

I would like to thank several people who helped me with this project. Rebekah Cordeiro, Natalie Owens, Hillary Olivier worked on the copper chemistry with me and Adam Stockhausen preformed stability tests on $56DMPAuCl_2^+$. Kenneth Hardcastle solved the crystal structures appearing in this paper. Thioredoxin reductase inhibition studies were preformed by Dr. Elias Arnér and Dr. Stephanie Prast at The Medical Nobel Institute for Biochemistry and cytotoxicity tests were carried out in the lab of Dr. Georgia Chen at Winship Cancer Center of Emory University. Dr. Matt Boone and Claney Pereira were invaluable in helping me in all aspects of my research and I would have gotten nowhere without them.

Finally, I would like to thank my advisors Frank McDonald and Jack Eichler who believed enough in me to give me a chance and showed me the ropes of chemistry. Dr. Eichler took a bright eyed freshman who thought he knew something and opened my eyes to just how complicated yet fulfilling research could be. Dr. McDonald built on that foundation, showing me everything that could be done in a lab. Without the two of you, I would be nowhere.

Table of Contents

III. A More Economical Synthesis of 4-Trimethylsilyl-2-butyn-1-ol

IV. Synthesis and Characterization of Copper(II) Paddlewheel Complexes Possessing Fluorinated Carboxylate Ligands

Figures and Tables

I. Synthesis and Characterization of 5,6-Disubstituted Phenanthroline-Gold(III)

Compounds as Anti-Tumor Agents

1. Introduction

Cancer ranks as the number two cause of death in the United States behind heart disease[1]. Treatments include radiation therapy, surgery, and chemotherapy, all of which have serious drawbacks. Because of the difficulties in developing targeted medications to treat cancers, platinum(II), gold(I), and gold(III) have become increasing popular metals for use in potential chemotherapeutics.[2-14] Since its approval in 1978 for the treatment of ovarian and testicular cancers, cisplatin (Figure 1.1) has been a first line therapy for several cancers, and continues to rank in the top three most used chemotherapeutics. However, its usefulness is limited by the small number of tumor types that respond to therapy; its relatively high toxicity, specifically to the kidneys; and the tendency of tumors to develop resistance. Cisplatin's solution chemistry is also a drawback since it has a low solubility in water and must be administered intravenously. Based on the success of cisplatin, thousands of Pt(II) compounds have been synthesized and 28 have entered human clinical trials. Out of these, only carboplatin has been approved for use in humans worldwide, although two other drugs, oxaliplatin and nedaplatin (Figure 1.1), have been approved in certain countries for use. All three of the second-generation Pt(II) drugs share the solubility and resistance problems of cisplatin, but are less toxic and can be administered in higher doses.[12]
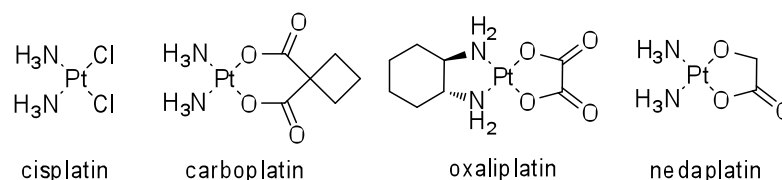
Figure 1.1: Structures of several Pt(II) drugs

Gold-based therapies are known to be of use in treating asthma, pemphigus, and rheumatoid arthritis (RA) and there is evidence to show their effectiveness in treating malaria, HIV, and cancer.[8] Gold has been used as a pro-drug in the treatment of RA since the 1970's, and it has been noticed that those undergoing treatment with auranofin (Figure 1.2), an Au(I) drug, are less likely to develop tumors than the general population.[11] However, there are only three Au(I) drugs still in use in the United States as of 1999, and only auranofin has been introduced in the previous thirty years.[8] The lack of drugs brought to market does not correlate to a dearth of research in the area of gold-based medicines. Recent studies have utilized several oxidation states for gold drugs including +I, +II, and +III.[8,11] Ligand systems employed in these reports include phosphines, thioglucose, bidentate thiolates, and charged thiols for Au(I); and bidentate amines, bidentate carboxylates, and imines have been utilized with Au(III). The difference in ligand choice is based on differences in the polarizability of Au(I) vs. Au(III).[11]
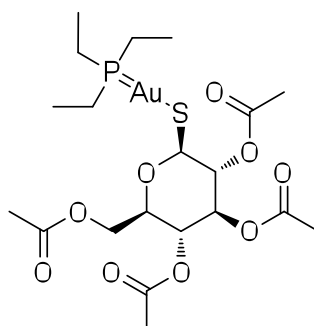
Figure 1.2: Structure of Auranofin

Since Au(III) and Pt(II) are isoelectronic, it was originally thought that they worked by the same mechanism; however, that theory has been disputed in recent years.[14] Cisplatin is known to work via binding to N-7 of guanine in DNA, creating a kink in the helix that prevents DNA transcription and replication and leads to cell death.[2,3] While

gold(III) is capable of binding to DNA, these interactions vary in their strength based on ligand and are usually quite weak.[14] Testing has shown that Au(III) prefers sulfur donating ligands such as glutathione and cysteine over nitrogen donating ligands in biological buffers. Several Au(III) complexes have been previously analyzed *in vitro* with calf thymus DNA and were found to alter its solution chemistry; however, the gold chromospheres were still present, and the binding affinities of the complexes was quite low, suggesting that the interactions are not redox, but rather, electrostatic in nature.[15] Au(III) drugs have also been shown to be effective on cisplatin-resistant tumors.[3,4] One study with Au(III) on both cisplatin sensitive and resistant leukemia cell lines found that there was little cross-resistance between the Pt(II) and Au(III) drugs.[16] A potential advantage of Au(III) drugs over Pt(II) drugs is the ability of Au(III) to enter the cell via an sulfhydryl-dependent membrane transport protein.[8] This difference would presumably increase the concentration of the active metal ions within the cytoplasm. A final difference is the ability of the chelated Au(III) centers to withstand reduction by biological anti-oxidants such as glutathione and ascorbic acid.[4,13] Until recently, there had been few biologically stable Au(III) compounds, but the use of bidentate ligands such as ethylenediamine and bipyridine have made these complexes viable treatment options.[3] The many recent discoveries in gold chemistry have led to renewed interest in the metal as a chemotherapeutic.

It has been proposed that Au(III) based chemotherapeutics work via mitochondrial impairment, specifically by inhibiting the mitochondrial enzyme thioredoxin reductase (TrxR) by binding to a selenocysteine residue found in the active site. TrxR has been identified as a potential target for drug therapies because of the role

of Trx in redox processes vital to mitochondrial function, cell signaling, and mitosis. TrxR is the only protein known to catalyze the reduction of the active disulfide bond in Trx and its over expression has been identified in several human cancers and has been associated with increased resistance to docetaxel in breast cancer therapy and decreased survival in colorectal cancers. TrxR inhibition by siRNA in mouse tumor cells has actually been shown to change the cells back to a normal phenotype and tumor growth and metastasis were reduced when the tumors were injected into a mouse model.[17]

Several previous studies have used complexes of bidentate nitrogen-donor ligands and tetrachloroaurate(III) salts in their molecular design because of the metal center's structural similarity to cisplatin. These Au(III) complexes have an $[AuCl_2]^+$ coordinated to two amine nitrogens, mimicking the d^8 square planar configuration of cisplatin. However, when there are substitutions α to the nitrogen, a neutral $AuCl_3$ will coordinate to a single amine.[4] Ligands utilized include dipyridoquinoxaline[7], dipyridophenazine[7], dipyrido(6,7,8,9-tetrahydro)phenazine[7], several different substituted porphyrins[9], phenanthroline (phen) with various substituents[4,6], phenanthroline-5,6-dione[6], and bipyridine (bipy) with various substituents[5,6]. In this study, that structural motif was continued with the use of 5,6-disubstituted phen ligands and tetrachloroaurate(III) salts; however, the resulting chloride complexes were converted to tetrafluoroborate salts *in situ* before isolation and characterization. The phen ligands used were 5,6-dimethyl- (**1,** 56DMP, Figure 1.3) and benzo[f]-1,10-phenanthroline (**2**, BP, Figure 1.3). One would expect that DNA interaction with the Au(III) center to be similar for all phen and bipy ligands if the binding sites are accessible from outside the helix, while the size of the ligand would play a role in the strength of binding if the bases are only accessible from

within the helix. If the molecule interacts via intercalation, then a larger aromatic system would presumably aid by increasing the attraction of π stacking. Since previously published evidence suggests that Au(III) is cytotoxic by non-mutagenic routes and approaches DNA from the ionic face rather than the aromatic face, there should be little difference in the DNA binding of the two compounds.
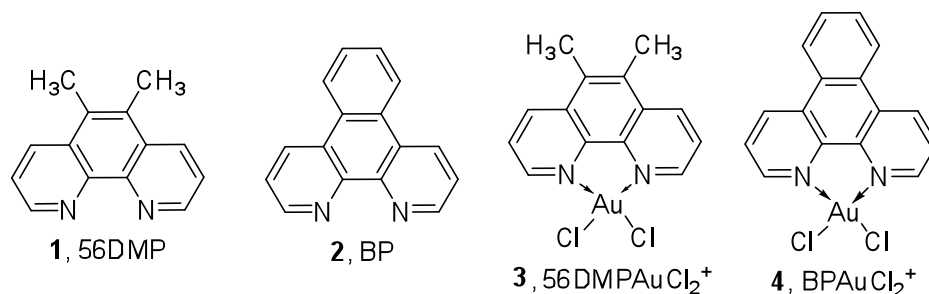
Figure 1.3: Ligands and complexes in this study

2. Results and Discussion

2.1. Synthesis and Characterization

BP and 56DMP were prepared from the corresponding phenylenediamine starting materials in moderate yield by the Skraup reaction (Scheme 1.1). Several papers[10,18] have described the synthesis of these ligands; however, we consistently obtained the products in lower yields than in previous reports. The purified ligands were then refluxed in methanol with $NaAuCl_4$ and $AgBF_4$ to give the desired gold complexes. The compounds were characterized by ^{1}H NMR, IR and UV-Vis spectroscopy and $56DMPAuCl_2^+$ was also characterized by X-ray crystallography (Figure 1.4). The complexes were tested for buffer stability, glutathione (GSH) and ascorbic acid stability, DNA binding, TrxR inhibition, and cytotoxicity against several human cancer lines.
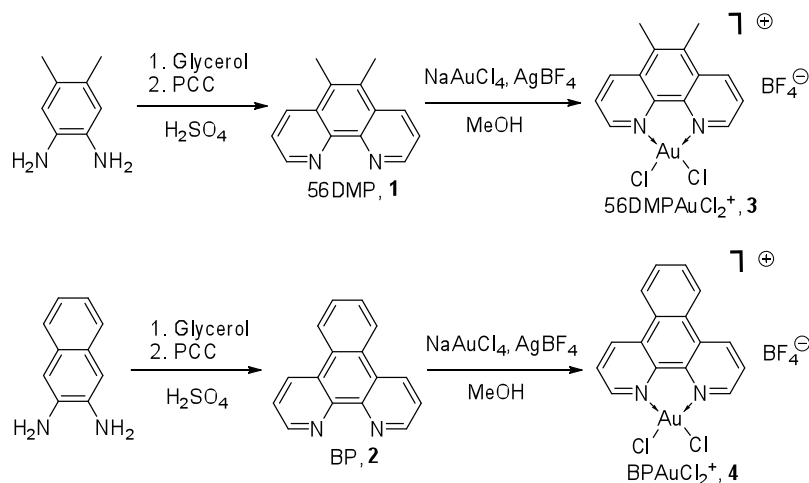
Scheme 1.1: Synthesis of phen-gold(III) complexes

Upon complexation with gold, the protons of the ligands became less shielded because the Au(III) ion pulls electron density out of the aromatic system. For 56DMP, the aromatic protons resonances moved downfield by 0.2-0.4 ppm and the methyl signal shifted by 0.07 ppm. A similar pattern was seen for the BP ligand upon binding to Au(III): one proton resonance shifted by 0.45 ppm upon complexation while the other resonances shifted by 0.1-0.25 ppm. PhenAuCl$_2^+$ shows shifts of 0.5 ppm for the least shielded proton and the two more shielded protons shift by 1 ppm.[7] The electron donating methyl groups of **3** and the larger aromatic system of **4** cause these complexes to show a smaller change than PhenAuCl$_2^+$ upon complexation.

The X-ray crystal structure of 56DMPAuCl$_2^+$ shows that it exists as a square planar d^8 compound, as expected. The N-Au bond lengths are 2.038(19) and 2.072(19) Å with a bite angle of 82.7(7)°. The chloride ions are more symmetrical with distances Au-Cl distances of 2.275(7) and 2.252 (7) Å and a bond angle of 89.1(3)°. The BF$_4^-$ anion resides between layers of 56DMPAuCl$_2^+$ units centered between the two methyl substituents and the extended structure consists of Au-π interactions that allow for

stacking of the layers. These observations all agree with previously characterized

bidentate amine complexes of Au(III).[7,19] The complex [PhenAuCl$_2^+$]Cl$^-$ shows N-Au

bond lengths of 2.033(8) and 2.056(8) Å with a bite angle of 82.0(3)° and Au-Cl

distances of 2.266(3) and 2.263(3) Å with a bond angle of 90.1(1)°. 56DMPAuCl$_2^+$ has a

less symmetrical coordination sphere around Au(III) than PhenAuCl$_2^+$, but both are

similar in their bite angles and Au-Cl bond lengths and angles. The difference in

symmetry could be due to the bulkier BF$_4^-$ counter anion in 56DMPAuCl$_2^+$.
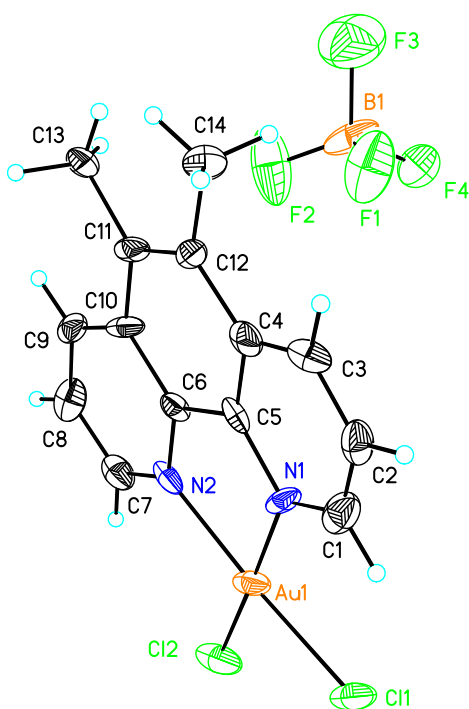
Figure 1.4: X-ray crystal structure of 56DMPAuCl$_2^+$

2.2. Biological Activity

2.2.1. DNA Binding

DNA binding activity was measured by incubating calf thymus DNA with the

gold complex for 24 hours followed by filtration through a 10,000 MW spin filter. A

UV-Vis spectrum was taken to detect the Au(III) chromophore at 350 nm. Greater

absorption indicates more Au(III) in the filtrate, and therefore, more unbound Au(III). A

control sample containing only gold solution was treated in a similar manner and used for comparison.

The binding studies show that only **4** binds strongly to DNA (Figures 1.5 and 1.6). The shoulder that appears in the spectrum of $BPAuCl_2^+$ at 275-325 nm in the control sample is not apparent in the +DNA sample. $56DMPAuCl_2^+$ shows a small decrease in absorbance upon ultrafiltration, but the logarithmic scale of absorbance means that a negligible amount of gold bound to DNA. In comparing these results to previously studied gold complexes, the binding of **4** seems to be relatively strong and the binding of **3** is average, although UV-Vis analysis does not quantify the results as reliably as other techniques. Using ICP-OES, one gold compound (2-(α,α-dimethylbenzyl)bipyAu) was found to bind 80% to DNA at a ratio of 10:1 DNA:Au(III).[14] A substantial change in DNA conformation was also noticed by CD for this compound. The strong binding of this compound correlated to a decrease in the Au(III) absorption in UV-Vis upon ultrafiltration. Based on this, it was thought that there was a change in the base stacking of DNA and that a very strong adduct was being formed. However, many other compounds showed interaction by CD that did not correlate to a decrease in absorption upon ultrafiltration, indicating that these interactions are electrostatic and reversible and the CD spectrum is thought to be due to slight changes in the helix.[5,14] Another study into the effects of ligand selection on DNA binding used three known intercalating agents with different size aromatic regions as ligands for Au(III) and did not find a correlation between the aromatic nature of the ligand and cytotoxicity, although the study did not specifically address DNA binding.[7] The large decrease in absorption of **4** upon ultrafiltration may indicate that the interaction

of BPAuCl$_2^+$ with DNA is not electrostatic in nature and a true chemical bond is created, possibly by an alteration of base stacking.
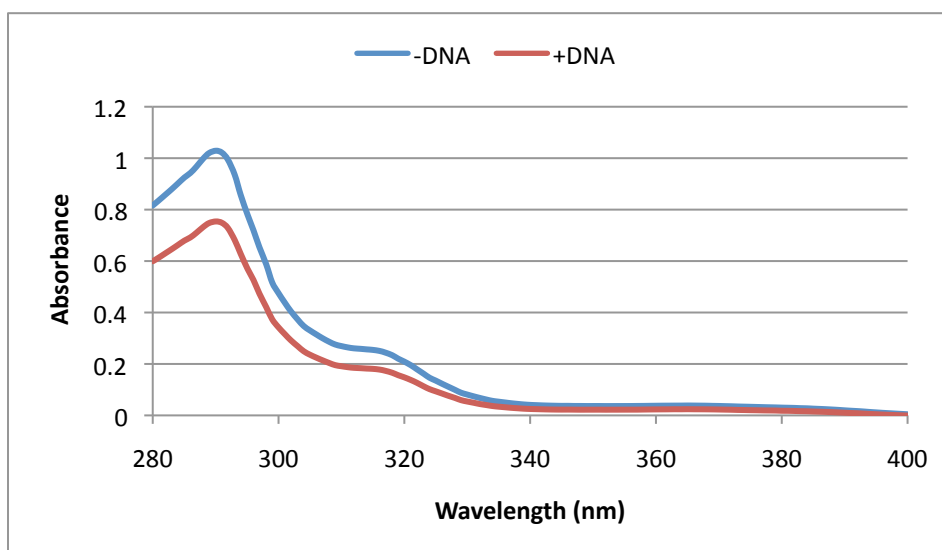
Figure 1.6: UV-Vis of filtrate of 56DMPAuCl$_2^+$ (**3**) with and without DNA (Performed by Adam Stockhausen)
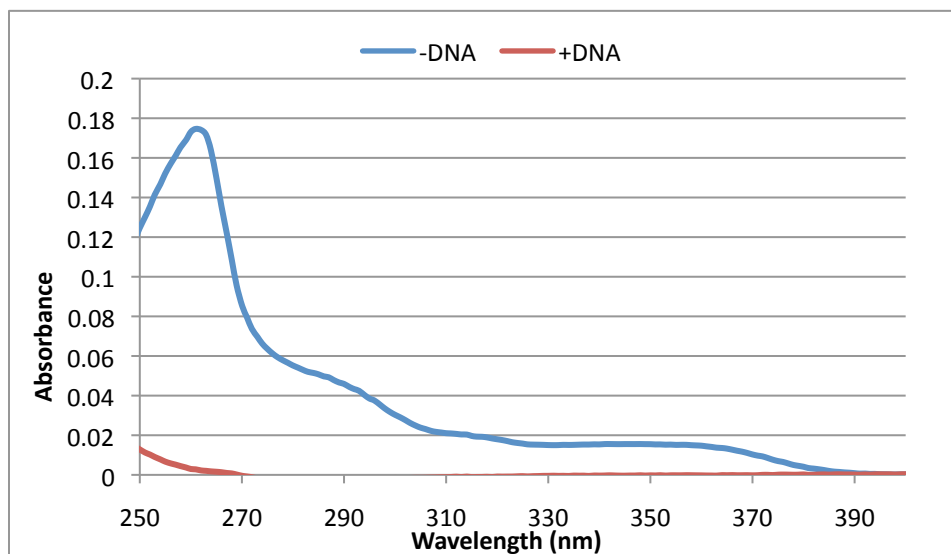
Figure 1.6: UV-Vis of filtrate of BPAuCl$_2^+$ (**4**) with and without DNA

2.2.2. TrxR Inhibition

Compound **3** (56DMPAuCl$_2^+$) showed much more activity against TrxR than compound **4** (BPAuCl$_2^+$) (Figure 1.7). 56DMPAuCl$_2^+$ had an IC$_{50}$ of 2.1±0.1 μM, comparable to the salts NaAuCl$_4$ and KAuCl$_4$ at 0.97±0.03 μM and 4.8±0.1 μM,

respectively. This is much lower than BPAuCl$_2^+$ at 79±2 μM (see Table 1.1). The reason for the large discrepancy is not known but could be due to sample degradation since a previous study of inhibition of TrxR by metals has shown that bidentate amine Au(III) complexes inhibit TrxR at an IC$_{50}$ on the order of 1 μM with values ranging from 0.21 to 1.42 μM. These values are significantly lower than cisplatin, which has an IC$_{50}$ of 36 μM, although auranofin has been shown to have an IC$_{50}$ of 20 nM.[20] These results seem to indicate that Au(III) has a much different reactivity towards proteins than Pt(II) or Au(I).
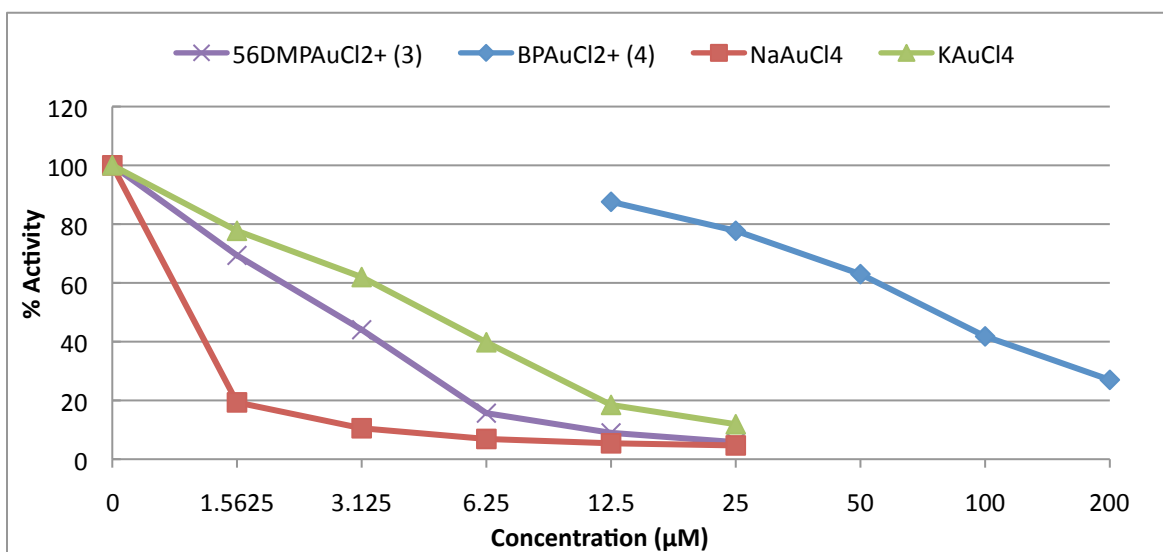
Figure 1.7: % activity of TrxR with varying concentrations of AuCl$_2^+$ complexes and controls (Performed by Dr. Elias Arnér and Dr. Stephanie Prast)

Substance	Mean	Standard Deviation	n
BPAuCl$_2^+$	79.5	2.12	2
56DMPAuCl$_2^+$	2.7	0.141	2
NaAuCl$_4$	0.975	0.0353	2
KAuCl$_4$	4.8	0	2

Table 1.1: TrxR inhibition IC$_{50}$ values for tested compounds

2.2.3. Cytotoxicity

Cytotoxicity studies on complexes **3** and **4** and the BP ligand show that all three are cytotoxic against cell lines A549, 886LN, Tu212, Tu686, and H1703 (Figures 1.8-

1.13 and Table 1.2). In all cases except one, both complexes and the BP ligand had lower

IC_{50} values than cisplatin with values ranging from 0.55-4.29 µM. The survival curves of

the BP ligand and $BPAuCl_2^+$ were almost identical in many of the cell lines tested and

were often both more effective than $56DMPAuCl_2^+$. The reason for the ligand's

cytotoxicity is not fully understood but could be due to a DNA interaction as phen

ligands are known to intercalate with DNA.[7] It is also possible that it sequesters metal

ions in the cytoplasm, leading to cell death. These results raise the possibility of

choosing ligands for gold(III)-based drugs that have cytotoxic properties for a synergistic

effect.

Many previous studies of Au(III) complexes used cell lines A2780/S and /R so a

direct comparison with complexes **3** and **4** is not possible.[5,7,14] However, all previously

reported complexes were less effective than cisplatin against the /S line and the majority

showed a similar cytotoxicity as cisplatin against the /R line. It is interesting to note that

the two complexes that were more effective than cisplatin against cell line A2780/R are

both monosubstituted at the 2 position of the bipy ring with a bulky aromatic group.

Complexes **3** and **4** seem to be more effective than previously reported compounds,

relative to cisplatin, but an absolute comparison is not possible with the current data.

All three compounds were much more effective than $NaAuCl_4$, which did not

show activity against the vast majority of cell lines. This suggests that the ligand is

essential for the Au(III) ion to enter the cell even though an transport protein is involved.

A study of many different Au(III) porphyrins found that lipophilicity is directly

correlated to cytotoxicity and cellular uptake with less polar complexes entering the cell

at higher levels and being more cytotoxic.[9] A different study used AuOH as a control

and found that it is more effective than many complexes against a cisplatin resistant cell line.[14] The reason for the difference in cytotoxicity between NaAuCl$_4$ and AuOH could be due to a difference in polarizability between the cations since the chloride ligands are known to exchange for OH ligands in aqueous solution[7] Au(I) would have more affinity for the thiol shuttle than Au(III), and thus, may be able to enter the cell more easily as a free ion.
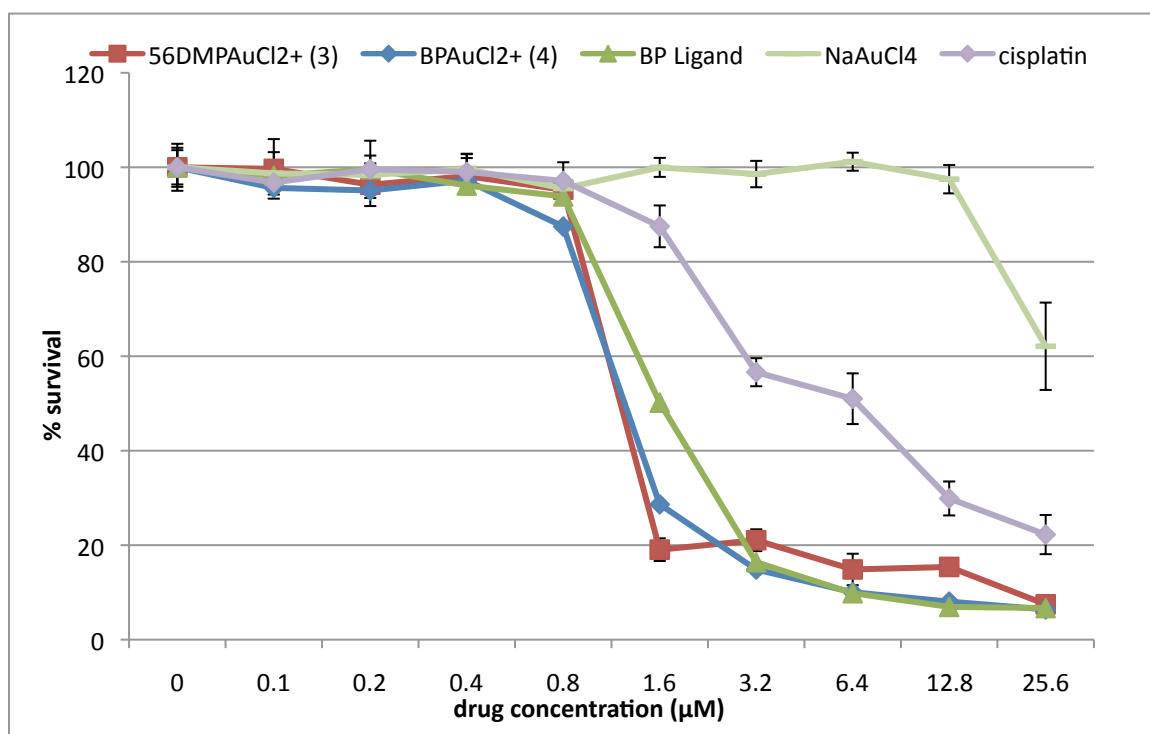
Figure 1.8: Concentration dependence of % survival for tested compounds on 886LN by SRB (3-16-09) (Preformed in the lab of Dr. Georgia Chen)
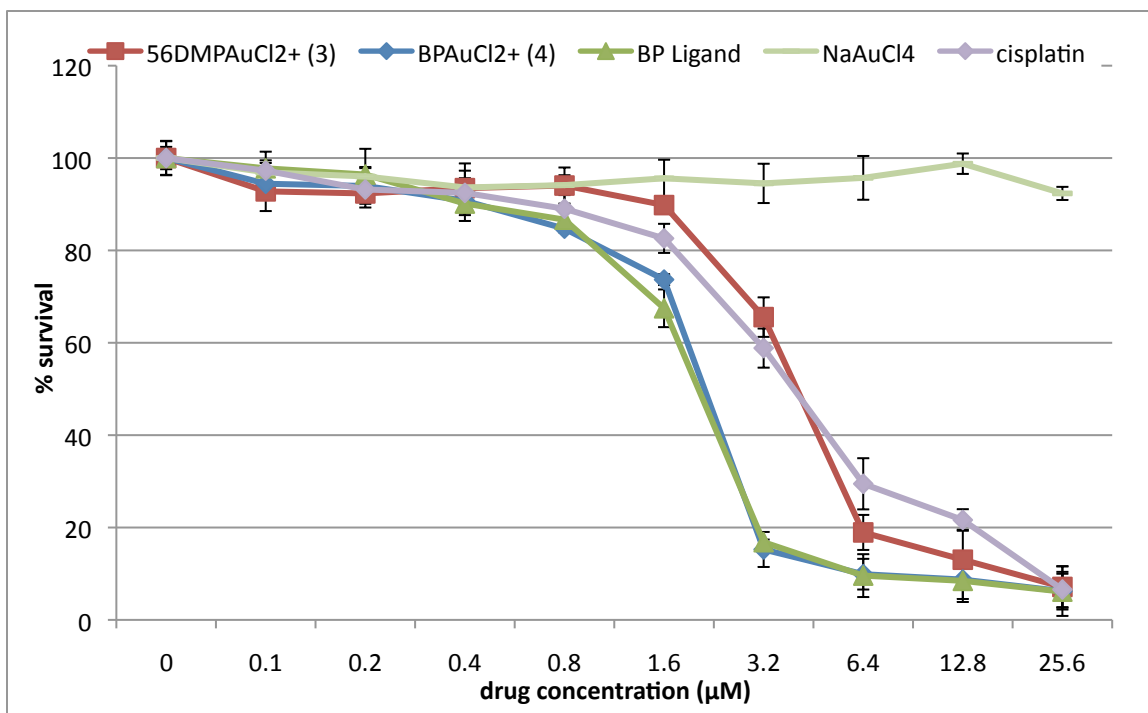
Figure 1.9: Concentration dependence of % survival for tested compounds on 886LN by SRB (3-23-09) (Preformed in the lab of Dr. Georgia Chen)
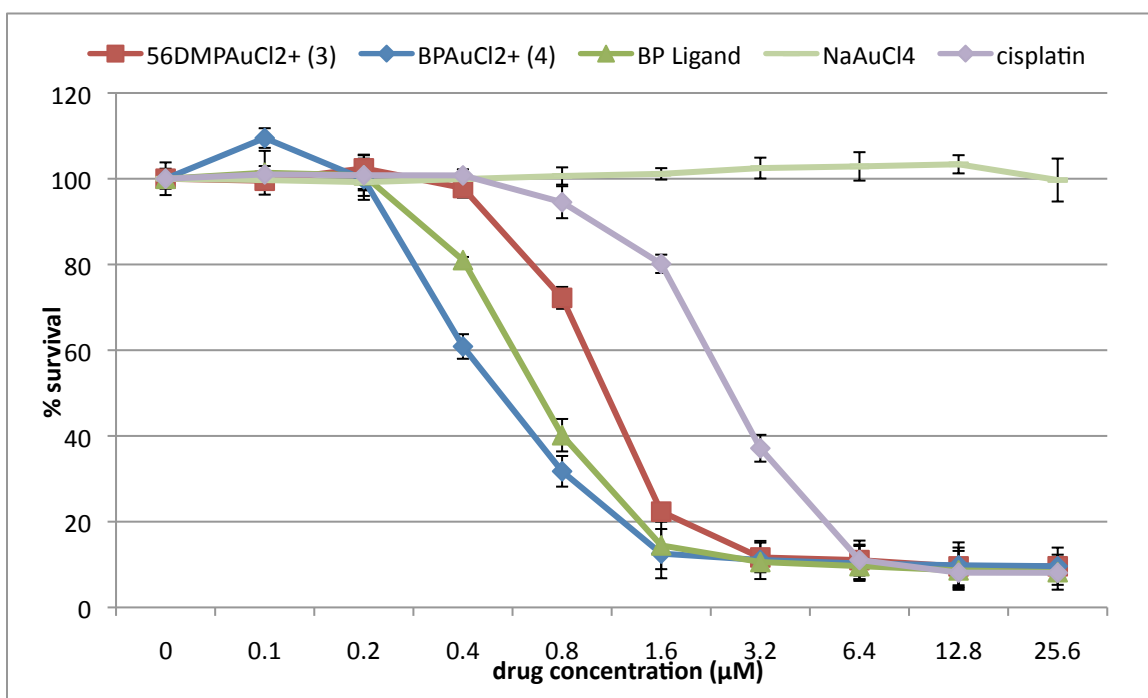
Figure 1.10: Concentration dependence of % survival for tested compounds on Tu212 by SRB (3-24-09) (Preformed in the lab of Dr. Georgia Chen)
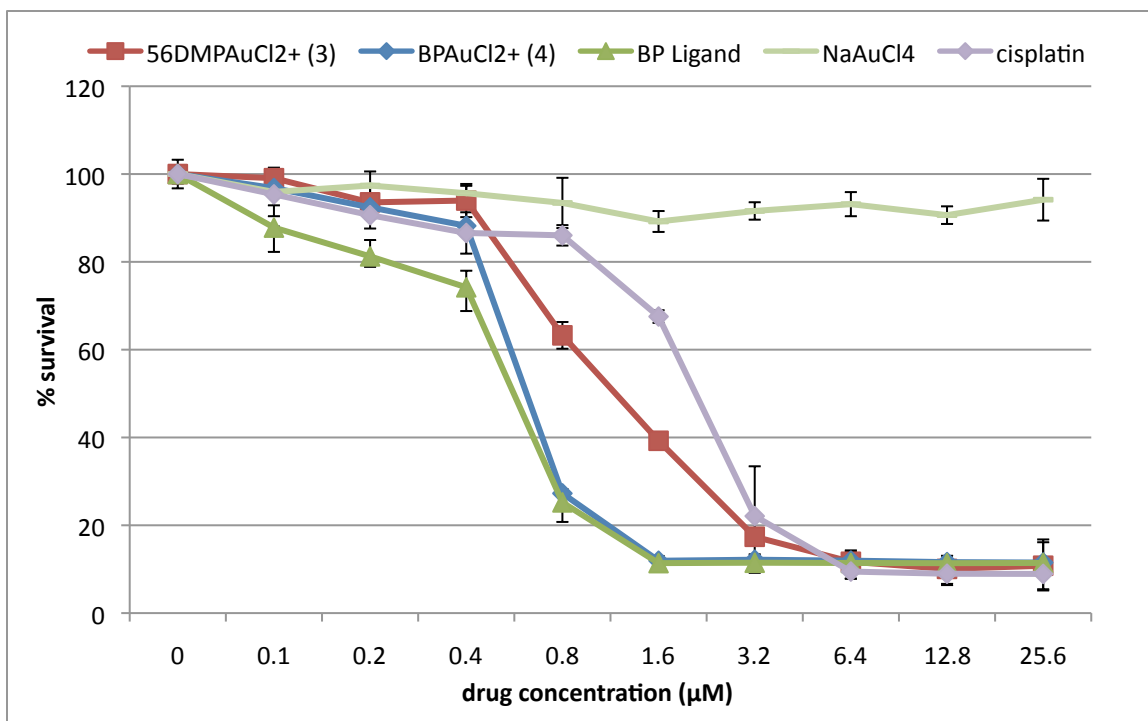
Figure 1.11: Concentration dependence of % survival for tested compounds on Tu212 by SRB (4-01-09) (Preformed in the lab of Dr. Georgia Chen)
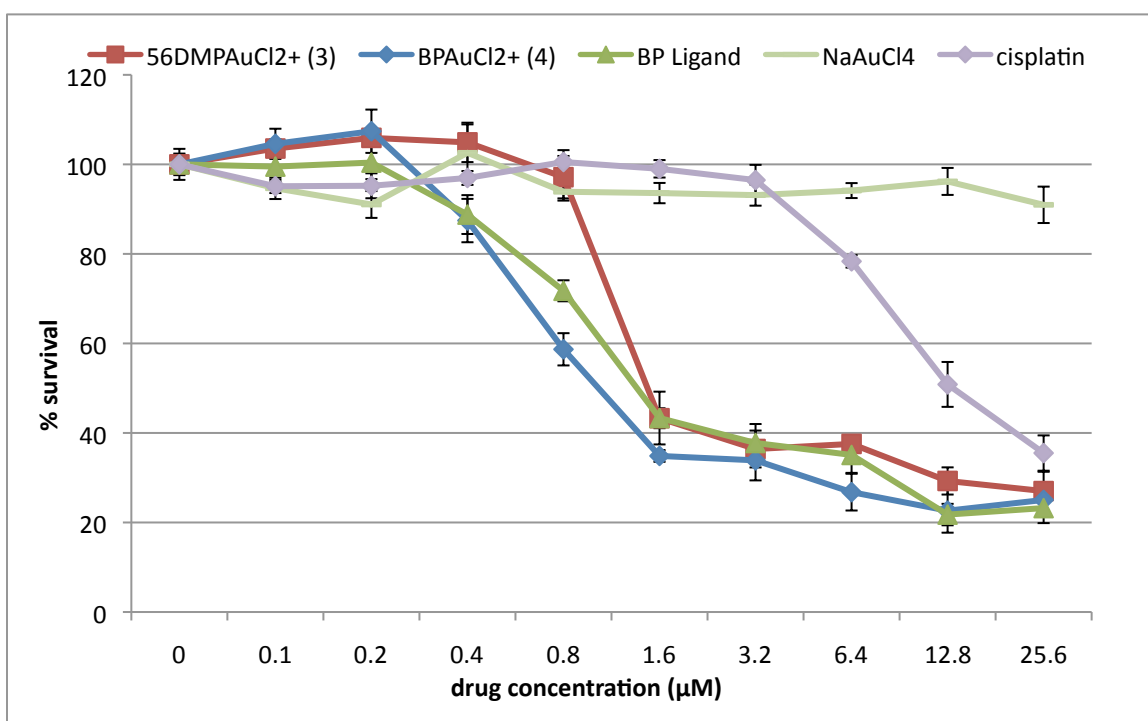
Figure 1.12: Concentration dependence of % survival for tested compounds on H1703 by SRB (Preformed in the lab of Dr. Georgia Chen)
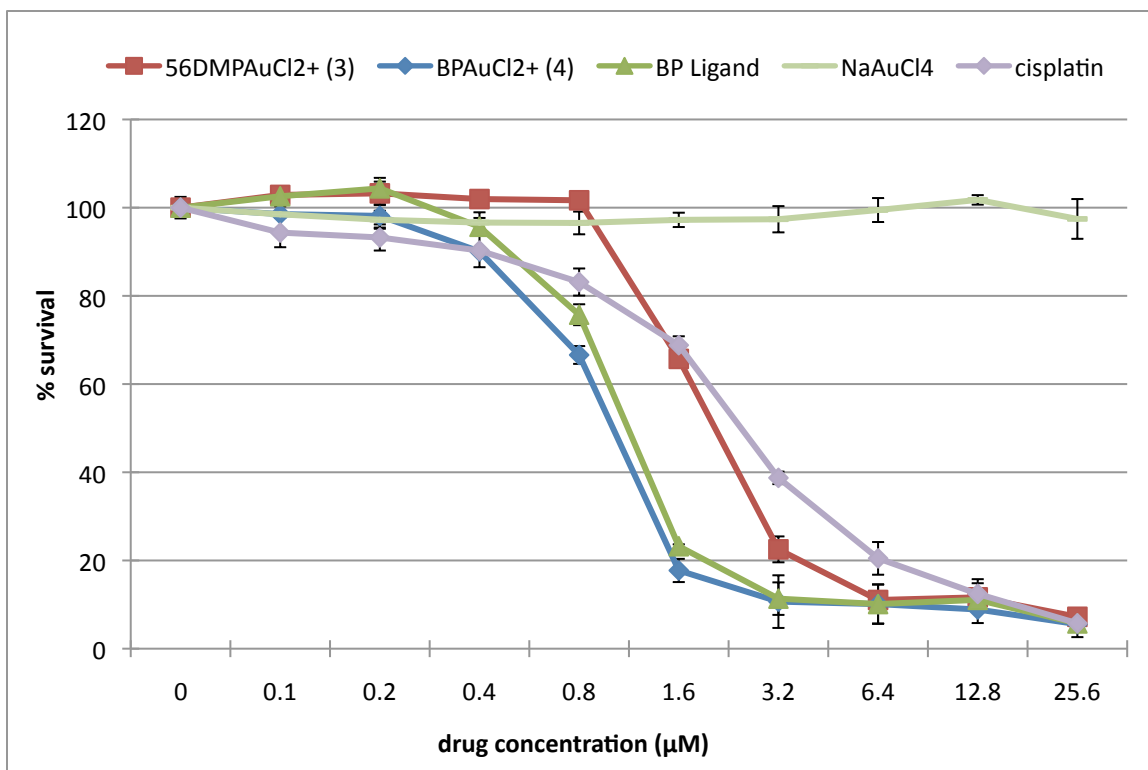
Figure 1.13: Concentration dependence of % survival for tested compounds on A549 by SRB (Preformed in the lab of Dr. Georgia Chen)

Compound	A549	886LN	Tu212	Tu686	H1703
$BPAuCl_2^+$	1.18	2.25	0.55	1.09	1.22
$56DMPAuCl_2^+$	2.14	4.29	1.15	1.6	1.31
BP Ligand	1.17	2.14	0.7	1.44	1.01
cisplatin	3.1	4.2	2.7	2.9	7.9

Table 1.2: IC_{50} values (µM) for tested compounds in various cell lines

2.4. Stability Studies

$56DMPAuCl_2^+$ showed good stability in buffer over a 24 hour period with a small change in UV-Vis in the first hour and little subsequent change in the next 23 hours (Figure 1.14). The initial change in absorption is probably due to Cl^- ion exchange and not a redox process. The absorptions observed can be tentatively assigned as a strong peak from n-π^* intra-ligand transitions at 288 nm, a shoulder from π-π^* intra-ligand transitions at 295-310 nm, and a weak absorption from ligand to metal charge transfer (LMCT) ranging from 335-390 nm. Upon addition of GSH or ascorbic acid to buffer

containing **3**, there is an immediate and dramatic change in UV-Vis spectra (Figures 1.15

and 1.16). A new absorption, presumably from colloidal gold^0 is seen at 520 nm and the

phen transitions show a marked increase while the LMCT absorption decreases. This

data is in agreement with previously published stability studies which found that most

Au(III) complexes are stable in buffer but have no redox stability.[7,14] Only one set of

redox stable gold(III) complexes have been reported and these use bulky alkyl groups in

close proximity to the metal.[21]
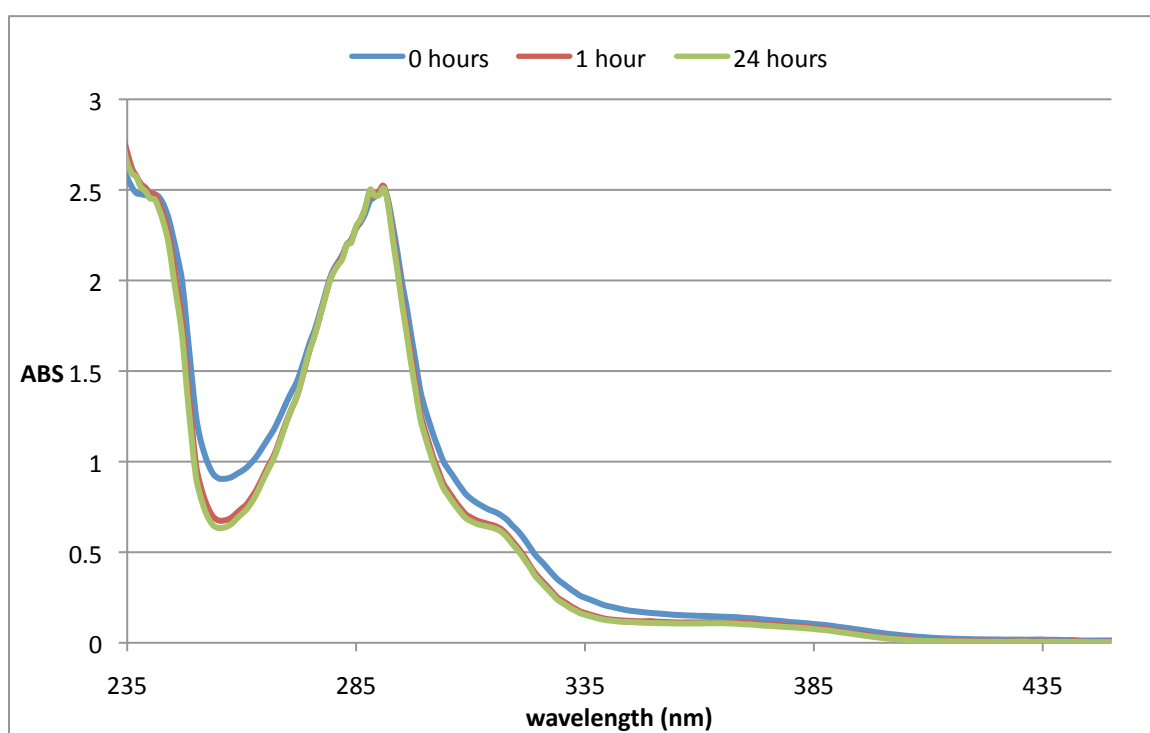
Figure 1.14: 24 hour buffer stability of **3** (56DMPAuCl$_2^+$) by UV-Vis (Performed by
Adam Stockhausen)
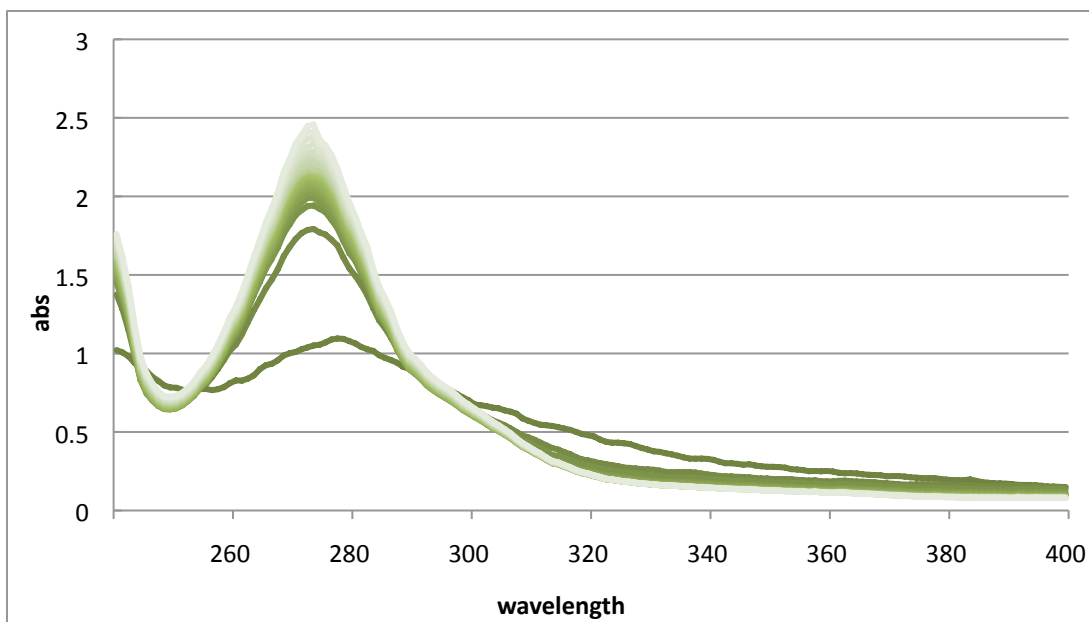
Figure 1.15: Hour by hour UV-Vis of reduction of **3** (56DMPAuCl$_2^+$) by GSH
(Performed by Adam Stockhausen)
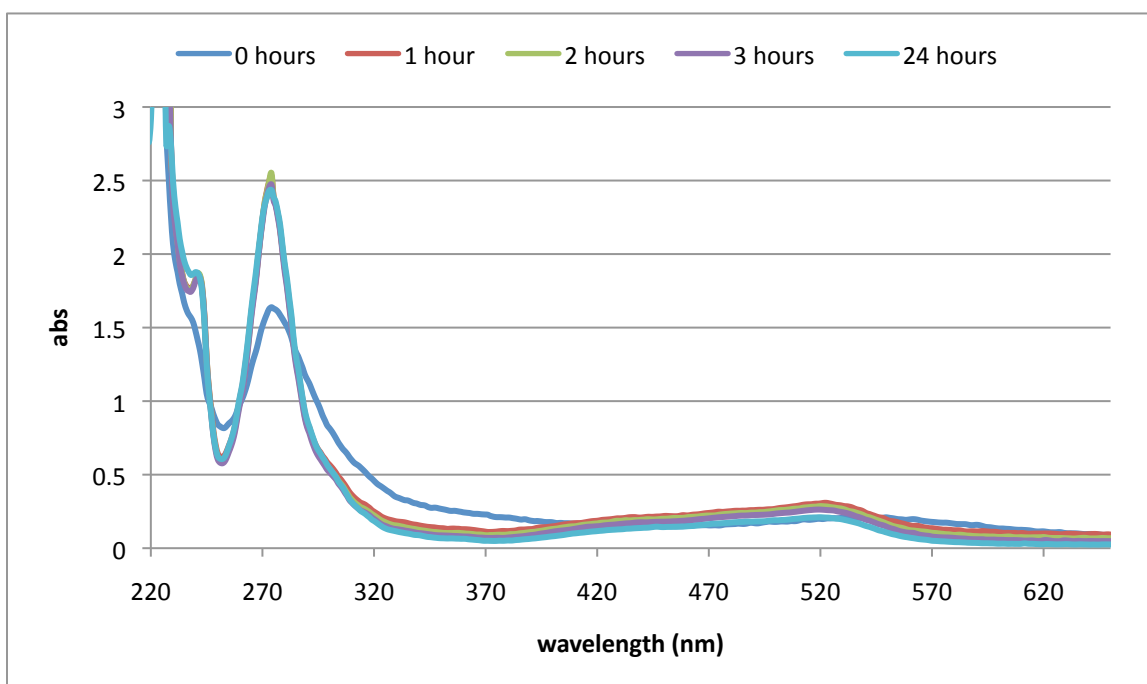
Figure 1.16: Ascorbic acid reduction of **3** (56DMPAuCl$_2^+$), monitored by UV-Vis
(Performed by Adam Stockhausen)

3. Conclusions

Two phenanthroline-based Au(III) complexes were synthesized, characterized and tested for biological activity. The compounds were stable in solution and BPAuCl$_2^+$

formed a strong DNA-Au(III) adduct with calf thymus DNA. From this study and others,
it seems neither sterics nor aromaticity of the ligands are decisive in DNA binding;
however, it is still not possible to determine the mechanism of DNA binding by these
complexes. Reduction with GSH and ascorbic acid resulted in an immediate and dramatic
drop in Au(III) concentration. When tested for cytotoxicity, both complexes were as or
more cytotoxic than cisplatin in all cell lines tested against. One complex,
$56DMPAuCl_2^+$ (**3**), showed significant TrxR activity while $BPAuCl_2^+$ (**4**) displayed much
less activity, though this experiment needs to be repeated to confirm the reliability of the
data. It seems from the data that there is no one cytotoxic pathway for Au(III) drugs.
Complexes **3** and **4** show similar cytotoxicity but **3** inhibits TrxR at a much lower
concentration. Further research into the mechanism of gold(III) induced cell death needs
to be preformed.

4. Experimental

4.1. General Experimental Procedures

Calf thymus DNA, DMSO-d_6, 4,5-dimethyl-1,2-phenylenediamine, 2,3-
diaminonaphthalene, pyridinium chlorochromate (PCC), silver tetrafluoroborate, sodium
tetrachloroaurate, and all cell culture reagents were purchased from Sigma-Aldrich, Inc.
All reagents were used without further purification, except that the calf thymus DNA was
made into a 1 mg/mL stock solution in 10 mM phosphate buffer (pH 7.4, 20 mM NaCl).
^{1}H NMR were recorded on a Varian Mercury spectrometer at 300 MHz in DMSO-d_6,
using the DMSO pentet at 2.50 ppm as an internal reference. UV-Vis were recorded on a
Cary 50 UV-Vis spectrophotometer and IR were recorded on a Varian Scimitar 800
Series IR spectrophotometer. Elemental analysis was preformed by Atlantic Microlab,

Inc.

4.2.1. 5,6-Dimethyl-1,10-phenanthroline[10,18](**1**, 56DMP)

Glycerol (4.35 g, 47.2 mmol) was added to concentrated sulfuric acid (15 mL)

and the solution was stirred at room temperature for ten minutes. 4,5-Dimethyl-1,2-

phenylenediamine was added (2.92 g, 21.5 mmol) in portions over ten minutes, and then

sulfuric acid (15 mL) was added. The solution was stirred at 75° C for 2 hours, or until

all solid had dissolved and the solution was dark and viscous. PCC (10.15 g, 47.2 mmol)

was added in portions over ten minutes. As the PCC was added, orange smoke evolved.

The solution was left to stir overnight (20 h) at 130-140° C. The solution was removed

from heat and allowed to cool to room temperature before cooling to 0° C in an ice bath.

The solution was basified (pH 9) with NaOH (50% aq.). The resulting precipitate was

filtered and dried *in vacuo*. The solid was extracted with EtOAc until the filtrate was

colorless (~4 L). The solution was concentrated by rotary evaporation to a volume of 500

mL. This solution was then flushed over alumina (basic, Brockmann grade III), dried

with MgSO₄, and filtered. The solvent was removed and the resulting brown solid was

dissolved in boiling benzene (10 mL). This solution was frozen and thawed. The solid

was filtered off to yield 272 mg (6%) of **1**. Identity was confirmed by NMR, which

matched the published spectrum.

4.2.2. Benzo[f]-1,10-phenanthroline[10,18] (**2**, BP)

BP was synthesized in analogous fashion to 56DMP using glycerol (3.20 g, 34.7

mmol), 2,3-diaminonaphthalene (2.50 g, 15.8 mmol), and PCC (7.47 g, 34.7 mmol).

Identity was confirmed by NMR, which matched the published spectrum.[10] Yield: 390

mg (11%)

*4.2.3. Dichloro-5,6-dimethyl-1,10-phenanthrolineaurate(III) tetrafluoroborate (***3***,*

56DMPAuCl$_2$$^+$)

NaAuCl$_4$ (0.230 g, 0.579 mmol) was added to a solution of MeOH (100 mL) and

1 (0.121 g, 0.579 mmol) in a round bottom flask. A precipitate was formed immediately

upon addition of **1**. The suspension was brought to reflux for 30 minutes and AgBF$_4$

(0.113 g, 0.579 mmol) was added. The reaction was refluxed overnight (16 h), cooled to

room temperature, and filtered though a fritted funnel packed with Celite to obtain a

yellow solution. The solvent was removed by rotary evaporation and the yellow solid

was washed with EtOAc. The solid was recrystallized from EtOH (20 mL) at 4°C to

yield 121 mg (39%) of **3**. ^{1}H NMR (DMSO, 300 MHz) ppm: 9.66 (dd, 2 H, *J*=5.6 Hz,

1.0 Hz); 9.44 (dd, 2 H, *J*=8.6 Hz, 1.0 Hz); 8.41 (dd, 2 H, *J*=8.5 Hz, 5.7 Hz); 2.89 (s, 6H);

IR (KBr pellet) cm^{-1}: 3400 (br), 3102, 3078, 2965, 2938, 2739, 2677, 2492, 2360, 2343,

1602, 1400, 1055; UV-Vis: λ_{max} 288 nm

For X-ray crystallography, a suitable crystal of **3** was coated with Paratone N oil,

suspended in a small fiber loop and placed in a cooled nitrogen gas stream at 173 K on a

Bruker D8 APEX II CCD sealed tube diffractometer with graphite monochromated Mo

K$_\alpha$ (0.71073 Å) radiation. Data were measured using a series of combinations of phi and

omega scans with 10 s frame exposures and 0.5^o frame widths. Data collection, indexing

and initial cell refinements were all carried out using APEX II[22] software. Frame

integration and final cell refinements were done using SAINT[23] software. The final cell

parameters were determined from least-squares refinement on 1489 reflections. The

structure was solved using direct methods and difference Fourier techniques

(SHELXTL, V6.12).[24] Hydrogen atoms were placed their expected chemical positions

using the HFIX command and were included in the final cycles of least squares with

isotropic U_{ij}'s related to the atoms ridden upon. All non-hydrogen atoms were refined

anisotropically. Scattering factors and anomalous dispersion corrections are taken from

the *International Tables for X-ray Crystallography.*[25] Structure solution, refinement,

graphics and generation of publication materials were performed by using SHELXTL,

v6.12 software.

4.2.4. Dichloro-benzo[f]-1,10-phenanthrolineaurate(III) tetrafluoroborate (4, BPAuCl$_2^+$)

NaAuCl$_4$ (0.247 g, 0.651 mmol) was added to a solution of MeOH (100 mL) with

2 (0.150 g, 0.651 mmol) in a round-bottom flask. The suspension was brought to reflux

for 30 minutes and AgBF$_4$ (0.12 g, 0.651 mmol) was added. The suspension was

refluxed overnight (18 h), cooled to room temperature, and filtered though a fritted

funnel to obtain a yellow solution. The solvent was removed by rotary evaporation and

the resulting solid was dissolved in CH$_3$CN. The solution was filtered though a fritted

funnel packed with Celite, and the solvent removed by rotary evaporation to give 110

mg (29%) of **4**. ^{1}H NMR (DMSO, 300 MHz) ppm: 9.71 (d, 2 H, *J*=6.2 Hz); 9.22 (d, 2 H,

J=4.7 Hz); 9.03 (dd, 2 H, *J*=6.1 Hz, 3.3 Hz); 8.22 (t, 2 H, *J*=4.1 Hz); 8.00 (dd, 2 H,

J=5.9, 3.0); IR (KBr pellet) cm^{-1}: 3400 (br), 3062, 1609, 1502, 1405, 1346, 1021, 812,

766; UV-Vis: λ_{max} 288 nm

4.3. DNA Binding

A solution of 5×10^{-5} M calf thymus DNA was made by combining 476 mL of 1

mg/mL DNA solution, 5 mg/mL gold-DMSO solution, and buffer (pH 7.4, 20 mM

NaCl) to make 3 mL total volume. The solution was incubated at 37°C for 24 hours in a

shaker at 150 rev/min. The solution was filtered though a 10,000 MW spin filter and a

UV-Vis spectrogram was taken. A control solution of 5×10^{-5} M gold compound in buffer was treated in a similar manner.

4.4. Thioredoxin Reductase Inhibition Studies[26]

For inhibition of TrxR, 50 nM recombinant rat TrxR1 (8.3 U/mg) was reduced by the addition of 250 µM NADPH to the assay buffer (50 mM Tris pH 7.5, 2 mM EDTA) and subsequently incubated 15 min at room temperature with increasing concentrations of the compounds. Two aliquots of 195 µL were subjected to a microtiter plate and 250 µM NADPH and 2.5 mM DTNB (Beta dystrobrevin) was added. Immediately, the DTNB reduction to TNB$^-$ was followed at 30°C for 5 min at 412 nm using the VersaMax (Molecular devices). A linear slope was calculated for the same 30 s interval of all samples within one run and the percentage of activity compared to enzyme incubated with assay buffer only was calculated for all treated samples.

4.5. Cytotoxicity Assays[27]

A sulforhodamine B (SRB) assay was performed following literature methods on cancer cell lines A549, 886LN, Tu212, Tu686, and H1703. Cells cultured in medium with 5% FBS were seeded in 96-well plates at a density of 4,000 cells/well 18 hours prior to drug treatment. Afterwards, compounds **2**, **3**, and **4** were added in a range of concentrations as single agents in various concentrations (0–30 µM), followed by incubation at 37°C and 5% CO_2 for 72 hours. Cells were fixed with 10% cold trichloroacetic acid for one hour. Plates were washed 5 times in water, air-dried, and then stained with 0.4% SRB for 10 min. After washing 4 times in 1% acetic acid and air-drying, bound SRB was dissolved in 10 mM unbuffered Tris base (pH 10.5). Plates were read in a microplate reader by measuring absorbance at 492 nm. Cell growth inhibition

was measured by determining cell density with sulforhodamine B assay at 72 hours after addition of the drugs. Percentage of inhibition was determined by comparison of cell density in the drug-treated cells with that in the untreated cell controls in the same incubation period. The percent survival was then calculated based upon the absorbance values relative to untreated samples. The experiment was repeated 3 times.

II. Towards the Synthesis of Conformationally Constrained Sphingosine Analogues

1. Introduction

Though cancer is the second leading cause of death in the United States, prostate cancer is the most common form of malignancy in men and the second deadliest. Prostate cancer is very treatable in its early stages, but once the cancer has metastasized and is androgen-independent, the survival rate drops to 33%.[28] In recent years, a class of compounds known as sphingolipids has emerged as lead compounds to treat these tumors. These compounds are metabolic products of sphingomyelin, which is found in the cell membrane and was once thought to only have a structural purpose. They are now known to affect cell signaling pathways and are believed to inhibit cell proliferation, induce differentiation, and increase apoptosis.

Sphingolipids have been tied to stress-induced apoptosis arising from both ionizing radiation and heat shock. Sphingosine has been shown to increase apoptosis in radiation-resistant prostate tumors.[29] A link has also been established between sphingomyelin metabolism and cancer development, especially in colorectal cancers.[30] The parent compound of sphingolipids, sphingosine ((2S,3R)-2-aminooctadec-4-ene-1,3-diol), has been shown to promote apoptosis; however, it has a primary alcohol that can be phosphorylated *in vivo* by sphingosine kinase (SPK) to form sphingosine-1-phosphate (S1P), which aids in tumor growth (Figure 2.1).[31] Sphingosine is capable of binding to DNA topoisomerase and can cause apoptosis in p53 resistant tumors.[30,32] In addition to inhibiting these two enzymes, it has been shown to inhibit Bcl-2 in HL-60 human leukemia cells[33] and Bcl-X$_L$ in DU-145 androgen-independent prostate cancer cells.[30] Conversely, S1P increases growth, differentiation, survivability, and motility. SPK

expression has been found to be a reliable indicator of cell fate by measuring the ratio of the intra-cellular levels of sphingosine and S1P.[34]
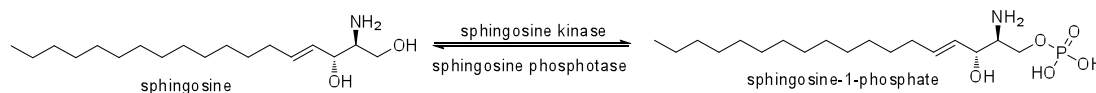
Figure 2.1: Sphingosine and S1P interconversion

Other sphingolipids have been shown to be of importance in influencing the cell cycle. Ceramide, a naturally occurring *N*-acyl sphingosine derivative is important in radiation induced apoptosis. Safingol ((2*S*,3*S*)-dihydrosphingosine, Figure 2.2) has been shown to cause apoptosis independent of p53 resistance, possibly by inhibiting PKC, of which it is capable of at μM concentrations.[31,32,35] It also increases *de novo* ceramide synthesis, but is thought to induce a different apoptotic pathway than sphingosine.[36] Safingol can reverse multi-drug resistance in doxorubicin (DOX) resistance cell lines, increase the activity of DOX, mitomycin C, and several other chemotherapeutics, increase the effect of DOX and cisplatin without increasing bone marrow or kidney toxicity, and in combination with DOX was the first PKC-specific drug cocktail to enter clinical trials.[35] Spisulosine ((2*S*,3*R*)-2-amino-3-hydroxyoctadecane, Figure 2.2) has been shown to cause Vero cells to become rounded and detach from the Petri dish *in vitro*, leading to apoptosis.[37]
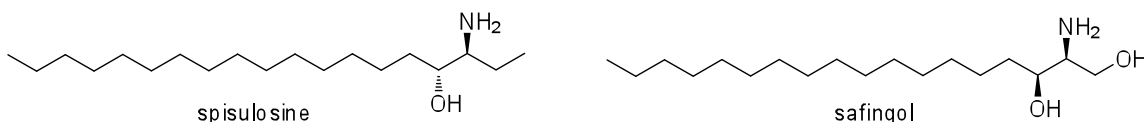
Figure 2.2: Two saturated sphingosine stereoisomers

Naturally occurring sphingolipids range in length from C_{12} to C_{30} and can have several different substitution patterns and stereochemistries at their hydrophilic head. A single naturally occurring sphingolipid[38] has been found to have 12 carbons; the halaminols[39] have 14; sphingosine, safingol, spisulosine, the crucigasterins,[40] and the

obscuraminols[41] have 18 carbons; the fumonisins[42] have a 20 carbon chain with two

methyl branches and 10 additional carbons in two esters; rhizochalin[43] has 28 carbons;

and the leucettamols have 30 carbons.[44] Sphingolipids of all lengths have been shown to

have biological activity, suggesting that tail length does not play an important role in

enzyme inhibition.

The common substitution pattern of all sphingolipids is a 2-amino-3-alcohol,

arising from their derivation from the amino acids serine, alanine, and glycine.[39] This

core pattern can be in the any of the four possible diastereomers $(2R,3R)$,[43] $(2R,3S)$,[45]

$(2S,3R)$,[41,46,47] or $(2S,3S)$[38,42,46,47] (Figure 2.3). The sphingolipids can also be found as

raecemic products of biosynthesis.[44] It appears that a certain configuration of the amino

alcohol portion is not necessary for biological activity as all of the above configurations

have shown some level of biological activity and ceramide has been shown to be

cytotoxic regardless of its absolute configuration.[30]

$(2R,3R)$ $(2R,3S)$ $(2S,3R)$ $(2S,3S)$
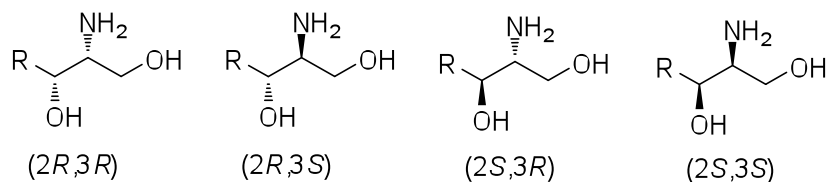
Figure 2.3: Possible stereoisomers of the hydrophilic head of sphingolipids

In addition to the common amino alcohol moiety, other positions on the chain can

be substituted. The most common are olefenic unsaturations in the hydrophobic tail.

These can be E or Z and occur at various positions in the chain including bond 4 in

sphingosine;[43] bond 5 in halaminol C,[39] bond 8 in clavaminol B; bond 11 in xestoaminol

A;[47] or bonds 9, 11, or 15, in obscuraminols D-F,[41] respectively. The unsaturations are

not limited to a single alkene in a molecule as the xestoaminols can have up to two

olefins,[47] obscuraminols can have up to four olefins,[41] and the leucettamols have six.[44]

The effect of these olefins is uncertain as they have been shown to be necessary for biological activity in ceramide, decrease biological activity in the clavaminols, and have little effect on the activity levels of sphingosine.[30,45]

A small number of sphingolipids have other functionalities (Figure 2.4). Rhizochalin, oceanapiside, and the leucettamols, collectively known as α,ω-bipolar sphingolipids, have a hydrophilic head on either end of the molecule.[43,44] Of these, rhizochalin and oceanapiside also have a ketone at carbon 11 and a sugar protecting the α-side hydroxyl group.[43] The fumonisins are the most heavily substituted sphingolipids with two carbon branches; four or five alcohols, of which two are esters with additional carboxylic acid groups; and a single amine.[42] The head of fumonisin is a 2*S*-amino-(3*S*,5*R*)-diol, which is another unique feature of this compound. The diversity of compounds which occurs naturally leads to many different possibilities for synthetic sphingolipids.
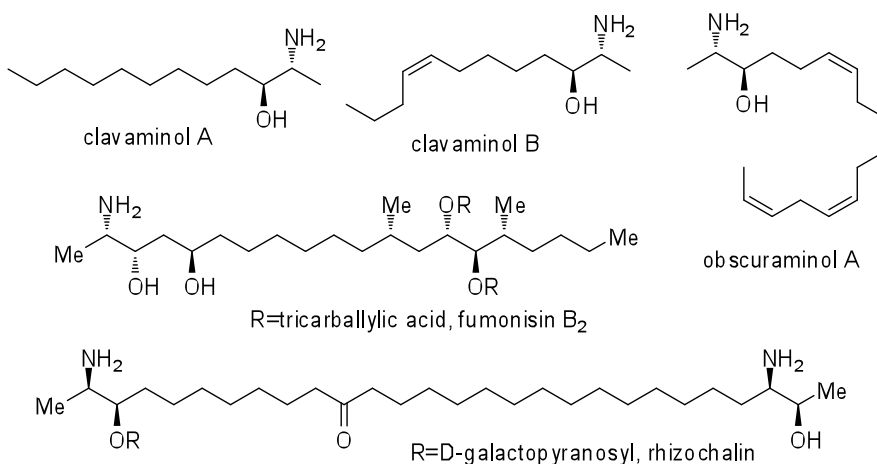
Figure 2.4: Various sphingolipids and their substitution patterns

The synthetic method used in this study is a three-piece convergent synthesis that allows for many different configurations of sphingolipids to be produced. The head and tail fragments are joined to a benzene spacer by epoxide-opening and Sonogoshira

coupling reactions, respectively (Scheme 2.1). This allows for different length heads and tails to be used and the position and regiochemistry (*ortho, meta, para*) of the benzene ring to be set based on the chosen terminal alkyne, azidoepoxide, and substituted benzene. The aromatic ring and unsaturations act to constrain the possible conformations of the hydrophobic tail to help elucidate the structure of the pharmacore. Because the coupled product has two alkynes, the unsaturation number of the final compounds can be altered and additional functional groups can be added. The epoxide synthesis can access all four diastereomers of the amino alcohol region based on *E/Z* regiochemistry of the starting alkene and the absolute stereochemistry of the tartrate ester used in the initial epoxidation. In this synthesis, a six-carbon terminal alkyne, a *meta*-benzene spacer, and a four-carbon epoxide were used to give a (2*R*,3*S*) amino alcohol.
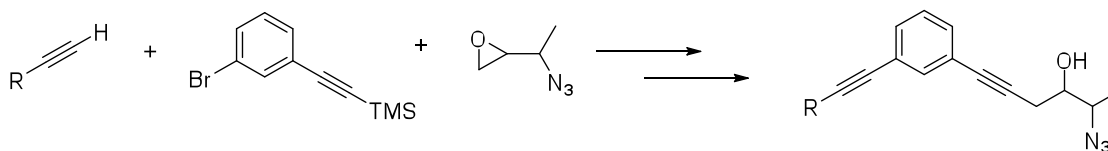
Scheme 2.1: Convergent synthesis of sphingolipids parent compound

Each parent diastereomer can give a family of 13 compounds via a divergent sequential oxidation/reduction method (Scheme 2.2). Compounds **B, C,** and **D** arise from reduction of the azide combined with no, partial, or complete hydrogenation of the alkynes to give spisulosine and halaminol analogues. Oxidation of the hydrophilic-side alkyne would give ketone **E** that would allow for several enigmol-type sphingolipids to be synthesized. These can have a varying number of unsaturations based on the hydrogenation catalyst and ketone reduction conditions. In all, this divergent method can yield 156 different compounds when all possible benzene spacers, diastereomers, and oxidation/reduction patterns are considered.
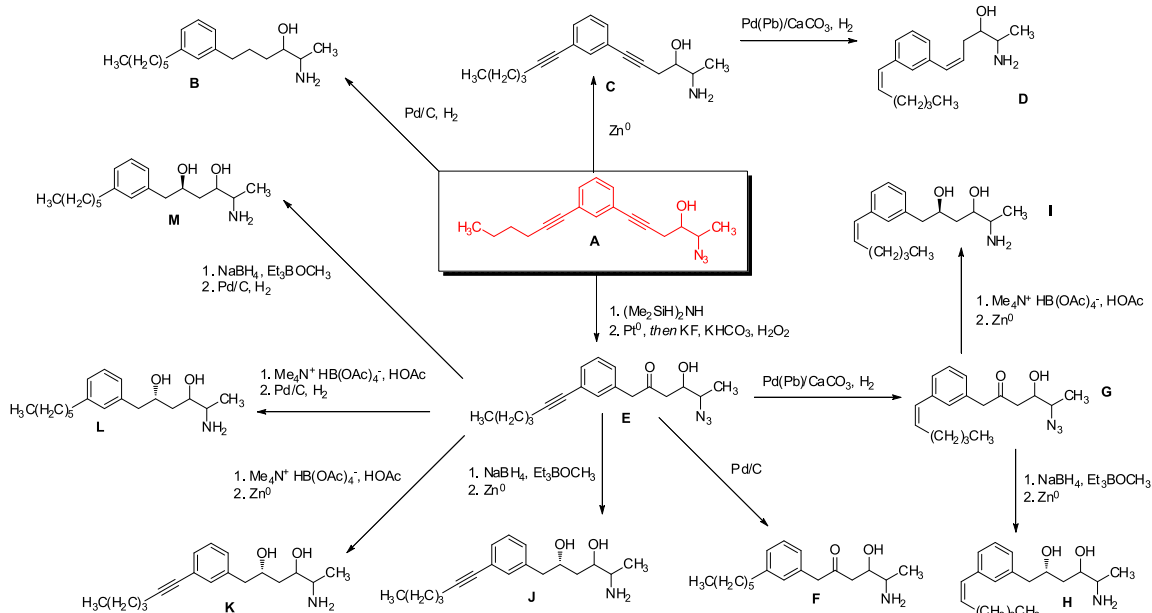
Scheme 2.2: Divergent synthesis of a family of sphingolipids

2. Results and Discussion

The synthesis of the hydrophilic section of the molecule proved to be rather difficult (Scheme 2.4). The initial hydrogenation to make allylic alcohol **1** was attempted with P2-nickel, which could not be removed from the substrate, so Lindlar's catalyst was used instead. While the conversion is a literature reaction, we observed that olefin **1** was isomerized to a mixture of isomers with the Z isomer dominating. This most likely happened in the course of hydrogenation; however, the olefenic isomerization was not apparent by NMR until after the Sharpless epoxidaton[48] when a mixture of epoxides was noted by NMR.

The epoxidation workup also proved to be problematic as epoxide **2** is volatile, which led to loss of compound when the solvents were initially removed by rotary evaporation. At first, the volatility was not realized because **2** still stains upon TLC of the crude residue, even though it cannot be detected by NMR. Using a more careful approach to the initial solvent removal, column chromatography was attempted on the

crude material; however, **2** proved difficult to separate from ethyl acetate as well. The

final purification method used a hexane/diethyl ether column which allowed for easier

solvent removal. Distillation was attempted, but was difficult and gave a product of

lower purity. A Mosher ester analysis was performed to determine enantiomeric excess,

but a comparison of the integrals of the major and minor peaks was not possible due to

peak overlap. The esters did separate the epoxide proton resonances allowing for the

assignment of the diastereotopic carbinol protons.

The azide insertion was a straightforward reaction with a simple and effective

workup.[49] Azide **3** was noted to be water soluble and several ether extractions were

required to fully remove it. There are several minor products of the reaction that could

not be separated by chromatography. By NMR, these are most likely regioisomers of the

desired product. They are presumably due to isomerization at the hydrogenation step,

low enantiomeric excess of the epoxidation, or the insertion not being fully selective for

the C-3 azide. Optimization of the preceding reactions will remove any side products

from previous steps and removal of the C-3 azide is not necessary because during the

subsequent epoxidation, the C-3 isomer may form an oxetane that will not react with

alkynyllithiums.
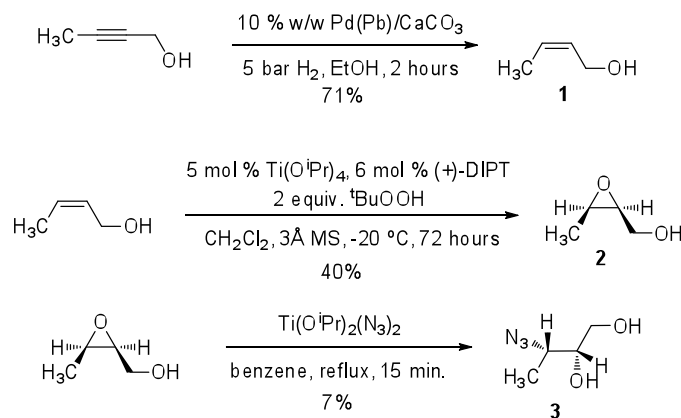
Scheme 2.3: Synthesis of the hydrophilic section

The Sonogoshira coupling was initially done by a modified version in toluene with Et$_3$N as the base; however, the original method of Sonogoshira[50] proved to be superior in this case. A silica gel pad was necessary to remove the catalyst but otherwise the workup was straightforward. The deprotection of the alkyne was also simple with K$_2$CO$_3$ giving better yields than tetrabutylammonium fluoride (Scheme 2.3) and no workup required.
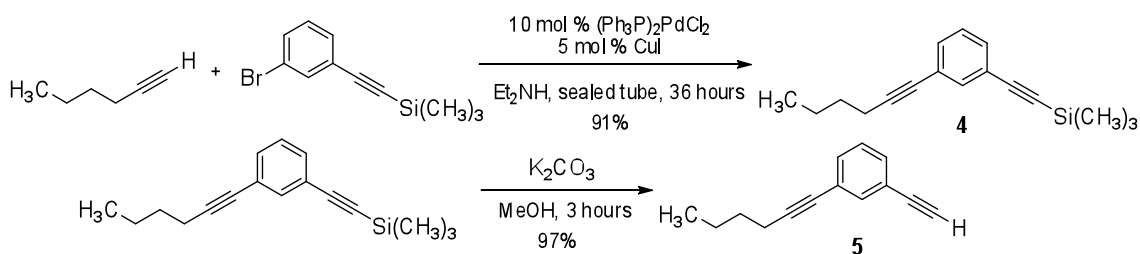
Scheme 2.4: Synthesis of hydrophobic sphingolipid tail

3. Conclusion

The method described is a three-part convergent synthesis of a family of sphingolipids. Although several steps must still be optimized, it should be able to give the desired compounds in good yield with high diastereoselectivity. Future optimization should explore hydrogenation catalysts along with the second coupling reaction, which was not attempted. This reaction would involve *in situ* creation of a second epoxide via an intramolecular S$_N$2 followed by addition of the alkynyllithiums and activation of the epoxide to give coupled secondary alcohol **6** (Scheme 2.4). Also, following the coupling, enantiomeric excess of alcohol **6** needs to determined and optical rotation measurements need to be made on precursors following confirmation of ee. Another route to these diastereomers is also possible starting with the *E* alkene, which is commercially available and seems to be easier to handle.[51] This would work via a Mitsunobu reaction on the

coupled product to invert the stereochemistry of the alcohol.
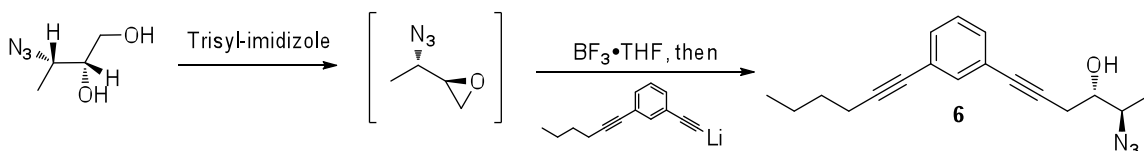
Scheme 2.5: Coupling of epoxide with alkynyllithium

4. Experimental

4.1. General Experimental Procedures

All reagents were purchased from Sigma-Aldrich and were used as received. Reagents were ACS reagent grade or better and solvents were HPLC grade. Solvents were dried with 3Å molecular sieves and stored under argon. ^{1}H and ^{13}C NMR were recorded in CDCl$_3$ on a Varian VNMR 400 at 400 and 100 MHz, respectively, except as noted. Tetramethylsilane was used as the internal standard. IR were recorded as a neat thin film on NaCl plates using a Gemini II FTIR. Mass spectroscopy was performed by APCI. Standard Schlenk techniques were used for air-sensitive portions of the synthesis

4.2. (Z)-But-2-en-1-ol (**1**)

2-Butyn-1-ol (25.00 g, 357 mmol, 26.28 mL), Lindlar's catalyst (2.50 g) and EtOH (250 mL) were added to a 500 mL pressure bottle. The bottle was placed in a Parr hydrogenation apparatus and purged twice with 5.1 bar H$_2$ gas. The bottle was shaken for 2.5 hours and removed from pressure. The solution was filtered through a Celite packed fritted funnel and the filtrate was removed by rotary evaporation to give crude product **1** as a yellow oil in 71% yield (18.36 g). The ^{1}H NMR matched published spectra[52] and the compound was used without further purification.

4.3. ((2S,3R)-3-Methyloxiran-2-yl)methanol (**2**)

A 1000 mL round bottom flask was charged with stir bar and flame-dried. The

flask was purged with argon and powdered 3 Å molecular sieves were added and the flask was purged with argon again. CH_2Cl_2 (500 mL) was added and the flask was placed in a dry ice-acetone bath and cooled to -78ºC. (+)-DIPT (3.57 g, 15.28 mmol, 3.21 mL), allylic alcohol **1** (18.36 g, 254.6 mmol), and $Ti(O^iPr)_4$ (3.62 g, 12.73 mmol, 3.72 mL) were added and the solution was stirred for 20 minutes. ^tBuOOH (5.5 M in decane, 509 mmol, 92.5 mL) was then added and the reaction was stirred for 3 hours at -70º C. The flask was then allowed to react at -20º C for 72 hours. After the reaction was complete by TLC, citric acid monohydrate (2.67 g, 12.73 mmol) was added and the reaction was diluted with Et_2O (100 mL). This was stirred for one hour, filtered, and the solvent was removed by rotary evaporation. The crude product was purified by flash column chromatography (2:1, Hexane:Et_2O, changing to Et_2O once product began to elute) to give product **2** in 40% yield (9.09 g). ^1H NMR ($CDCl_3$, 400 MHz) ppm: 3.86 (dd, 1 H, J=12.1 Hz, 4.1 Hz); 3.70 (dd, 1 H, J=12.1 Hz, 6.8 Hz); 3.16 (m, 2 H); 1.33 (d, 3 H, J=5.6 Hz); ^{13}C NMR ($CDCl_3$, 100 MHz) ppm: 60.9, 56.9, 53.0, 13.6; IR (neat) cm^{-1}: 3413, 2977, 2935, 2881, 1739, 1041, 875; HRMS (APCI): m/z calcd. for $C_4H_9O_2$ $(M+H^+)$ 89.05971, found 89.05959

For *in-situ* determination of the enantiomeric excess of **3** by Mosher ester analysis, an NMR tube containing the alcohol **3** (ca. 5 mg) and pyridine-d_5 (2 - 3 drops) was dissolved in $CDCl_3$ (0.6 mL), and 2 - 3 drops of (*S*)- or (*R*)-methoxy(trifluoromethyl)phenylacetyl chloride were added. The tube was gently shaken and then allowed to stand overnight, to afford a solution of the (*R*)- or (*S*)-MTPA ester, respectively. NMR data (600 MHz, $CDCl_3$) are summarized in Table 2.1.

Proton	Alcohol	(*R*)- Mosher Ester	(*S*)- Mosher Ester
H_a	3.86	4.43	4.52
H_b	3.70	4.11	4.36
H_c	3.16	3.19	3.21
H_d	3.16	3.13	3.14
H_e	1.33	1.32	1.30

Table 2.1: NMR data (ppm) for Mosher ester analysis

4.4. (2R,3S)-3-Azidobutane-1,2-diol (**3**)

A 500 mL three-neck round bottom flask equipped with a reflux condenser was charged with stir bar, flame dried, and purged with argon. Dry benzene (100 mL) was added along with Ti(O^{i}Pr)$_4$ (9.685 g, 34.1 mmol, 9.98 mL) and azidotrimethylsilane (7.861 g, 68.2 mmol, 9.05 mL). The solution was brought to reflux for 18 hours. To the refluxing suspension was added epoxy alcohol **2** (3.00 g, 34.1 mmol) and the suspension turned clear. The reaction was left at reflux for 15 minutes and then allowed to cool to r.t. Benzene was removed by rotary evaporation, the oil was diluted with Et$_2$O, 5% H$_2$SO$_4$ was added, and the solution was stirred for one hour. The layers were separated and the aqueous layer was extracted with Et$_2$O. The combined organic layers were evaporated to give the crude product. The product was purified by flash column chromatography in 1:1 Hex:EtOAc to give azidodiol **3** in 7 % yield (0.1036 g) as a 58:42 mixture of diastereomers. ^{1}H NMR (CDCl$_3$, 400 MHz) ppm: 4.15-4.11 (m, 0.9 H); 3.87 (dt, 0.4 H, *J*=6.3 Hz, 3.9 Hz) 3.76-3.63 (m, 2.3 H), 1.23 (d, 1.8 H, *J*= 6.6), 1.19 (d, 1.5 H, *J*=6.7 Hz); ^{13}C NMR (CDCl$_3$, 100 MHz) ppm: 81.1, 73.9, 73.8, 64.3, 63.5, 15.0, 13.8; IR (neat) cm^{-1}: 3367, 2937, 2931, 2507, 2105, 1639, 1261, 1056, 867

4.5. ((3-(Hex-1-yn-1-yl)phenyl)ethynyl)trimethylsilane (**4**)

A 100 mL Schlenk flask was charged with a stir-bar and flame dried. The flask was purged with argon and Et$_2$NH (20 mL), ((3-bromophenyl)ethynyl)trimethylsilane

(1.00 g, 3.95 mmol, 1.19 mL) , $(Ph_3P)_2PdCl_2$ (0.277 g, 0.395 mmol), CuI (0.037 g, 0.198 mmol), and 1-hexyne (0.389 g, 4.73 mmol) were added sequentially. The flask was sealed and left 48 hours. In the first few minutes of the reaction the solution went from yellow to green to brown and remained brown for the duration. After completion, the solvent was removed by rotary evaporation and water was added to the remaining residue. The aqueous later was extracted (3x25 mL) with Et_2O. The combined organic fractions were dried with $MgSO_4$, filtered, and the solvent was removed by rotary evaporation. This crude yellow oil was purified by flash column chromatography with hexanes to give silane **4** in 91 % yield (0.9089 g). ^1H NMR ($CDCl_3$, 400 MHz) ppm: 7.50 (s, 1H); 7.34 (dd, 2 H, J=9.2 Hz, 8.3 Hz); 7.21 (dd, 2 H, J=7.7 Hz, 7.7 Hz); 2.40 (t, 2 H, J=7.0 Hz); 1.59-1.41 (m, 4 H) 0.96 (t, 3 H, J=7.3 Hz), 0.25 (s, 3 H); ^{13}C NMR ($CDCl_3$, 100 MHz) ppm: 135.2, 131.7, 131.1, 128.4, 124.5, 123.4, 104.7, 94.9, 91.4, 79.9, 31.0, 22.2, 19.3, 13.8, 0.2; IR (neat) cm^{-1}: 3062, 2958, 2931, 2869, 2229, 2159, 1592, 1473, 1249, 1180, 844; HRMS (APCI): m/z calcd. for $C_{17}H_{22}Si$ ($M+H^+$) 255.1563, found 255.1559

4.6. 1-Ethynyl-3-(hex-1-yn-1-yl)benzene (**5**)

Silane **4** (0.9089 g, 3.57 mmol) was added to K_2CO_3 (0.4937 g, 3.57 mmol) in MeOH (20 mL) and the reaction was stirred for 3 hours. MeOH was removed by rotary evaporation and the residue was dissolved in EtOAc and filtered. The solvent was removed by rotary evaporation to give substituted benzene **5** in 97 % yield (0.627 g). ^1H NMR ($CDCl_3$, 400 MHz) ppm: 7.51 (s, 1 H); 7.38 (dd, 2 H, J=7.0 Hz, 7.0 Hz); 7.25 (dd, 2 H, J=7.7 Hz, 7.7 Hz); 3.06 (s, 1 H), 2.40 (t, 2 H, J=7.0 Hz); 1.66-1.43 (m, 4 H) 0.96 (t, 3 H, J=7.3 Hz); ^{13}C NMR ($CDCl_3$, 100 MHz) ppm: 135.1, 131.9, 131.1, 128.3, 124.4,

122.4, 91.3, 83.0, 79.6, 77.6, 30.7, 22.0, 19.1, 13.7; IR (neat) cm^{-1}: 3297, 3062, 2958, 2931, 2869, 2229, 2109, 1592, 1473, 894, 794; HRMS (APCI): m/z calcd. for C$_{14}$H$_{15}$ (M+H$^+$) 183.1168, found 183.1165

III. A More Economical Synthesis of 4-Trimethylsilyl-2-butyn-1-ol

1. Introduction

The first synthesis of 4-trimethylsilyl-2-butyn-1-ol was reported by Mastalerz in

1984[53]. This reagent has since been used in the synthesis of 2-tributylstannyl-1,3-

dienes[54]; 3,4-di, 2,4,5-tri, and 2,3,4-tri substituted tetrahydrofurans[55,56]; bridged

azabicyclic systems[57]; (±)-neolemnanyl acetates[58]; and following addition to another

carbon chain the TMS group can be eliminated to form an allene.[59,60] This last property

of the reagent was utilized in the first generation total synthesis of abudinol B.[61] Because

Mastalerz's starting material, 2-trimethylsilyl-1-propyne is relatively expensive, our

synthesis was developed to give the desired product in similar yields with a much less

expensive starting material. By double-deprotonation of 2-butyn-1-ol at the hydroxyl

group and alkyne followed by addition of 2 equivalents chlorotrimethylsilane, it is

possible to get the TMS-protected alkyne which can be easily O-desilylated with acetic

acid to give the desired compound in moderate yield (Scheme 3.1). While Mastalerz's

synthesis is more atom efficient, our method is much more cost effective.
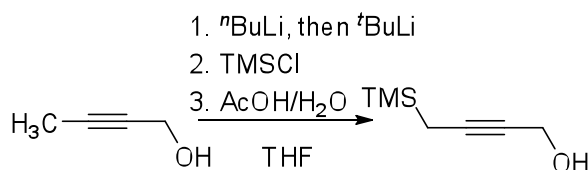
Scheme 3.1: Synthesis of 4-TMS-2-butyn-1-ol

2. Discussion

The product, 4-TMS-2-butyn-1-ol, was produced consistently in 35-40% yields

following optimization. Better yields were noted when saturated aqueous ammonium

chloride was used to neutralize lithium hydroxide before adding acetic acid to the

reaction; however, freshly distilled chlorotrimethylsilane did not improve yields. Our

lower yields are most likely due to the multiple sites for deprotonation on 2-butyn-1-ol, which may give rise to several regioisomers of the desired product. The unknown side product formed in the course of the reaction is probably one of these compounds, owing to the observed trimethylsilyl substituent by NMR and the similar boiling points of the two products.

Distillation was the preferred method of purification, but a distillation head of 25 cm was required to separate the two products. Column chromatography at the ether stage would have eliminated the need for a long distillation path since the unknown impurity has an R_f similar to the alcohol. However, we chose the greener and more cost effective method of purification.

3. Procedure

4-Trimethylsilyl-2-butyn-1-ol: 2-Butyn-1-ol (98%), tetrahydrofuran (≥99%), chlorotrimethylsilane (98%), *tert*-butyllithium (1.7 M in pentane), and *n*-butyllithium (2.5 M in hexanes) were purchased from Sigma-Aldrich. The THF was dried with and stored over 3Å molecular sieves under argon. Before each reaction, the water content of the THF was determined with a Denver Instruments Model 275KF Colorimetric Karl-Fischer Titrator to ensure less than 10 ppm water. All other reagents were used without further purification. Standard Schlenk techniques were used for air-sensitive portions of the synthesis. All temperatures are internal.

A three neck, 500 mL round-bottom flask, equipped with two septa on the outside necks and a low-temperature thermometer on the middle neck, was charged with a stir bar and flame-dried. The flask was purged with argon and of THF (150 mL) and 5.34 mL of 2-butyn-1-ol (5.00 g, 71.3 mmol) were added. This solution was cooled to -70° C

with a dry ice-acetone bath. Once cooled, *n*-BuLi (28.5 mL, 71.3 mmol, 1.0 equiv), was

added at 60 mL/h by syringe pump and the solution was allowed to stir for 5 minutes.

Next, *t*-BuLi (46.2 mL, 78.5 mmol, 1.1 equiv) was added at 60 mL/h by syringe pump.

As the alkyllithiums were added, the solution developed a yellow color. The dry ice was

removed from the acetone bath, and reaction was allowed to warm to 0° C (2-3 hours)

and stirred in an ice bath for 20 minutes. A precipitate began to form in the solution at

-45° C and the solution became cloudier as it warmed. The reaction vessel was then

recooled to -70° C and TMSCl (18.0 mL, 15.5 g, 142 mmol, 2.0 eq) was added by

syringe pump at 45 mL/h to the solution of the dianion intermediate. As the first

equivalent of TMSCl was added, the precipitate dissolved and the solution lost its color.

As the second equivalent was added, the solution became a light green color. The

reaction flask was left to warm to room temperature and stir for overnight 16-18 hours.

The next morning, the reaction mixture was cloudy and cream-colored. The

reaction was quenched with saturated aqueous NH_4Cl (100 mL) and the biphasic mixture

was stirred vigorously for 5 minutes. Water (100 mL) was added to dissolve the

precipitate salts, and the mixture was stirred for a further 25 minutes. Et_2O (100 mL) was

added to dilute the organic layer and the layers were separated. The aqueous layer was

extracted with Et_2O (2x25 mL) and the combined organic layers were concentrated to

~75 mL by rotary evaporation (35° C, 210 mmHg). A stir bar was placed in the flask,

and 15 mL of 8.73 M (50% aqueous) AcOH was added to cleave the trimethylsilyl ether.

The reaction was monitored by TLC. When complete, the reaction was basified with

saturated aqueous $NaHCO_3$ in portions. The layers were separated and the organic layer

was collected. The aqueous layer was extracted with Et_2O (2x50 mL), the combined

organic layers were washed with brine (1x100 mL), and dried with $MgSO_4$. After filtration, the crude mixture was concentrated under reduced pressure via rotary evaporation to give a yellow oil.

This crude product was purified by vacuum distillation. A standard vacuum distillation setup consisting of oil bath, flask with compound, distillation head and condenser, and udder connected to four 50 mL round bottom flasks was used. The first distillate consisted of TMSOH which was distilled at 45-55°C (150 torr), an impurity was the second distillate, obtained at 119°C, followed closely by the desired compound at 123°C. The product, 4-trimethylsilyl-2-butyn-1-ol, was obtained in 35-40 % yield (3.5-4.0 g).

2.1 Characterization Data

^{1}H NMR (CDCl$_3$, 300 MHz) ppm: 4.22 (t, 2H, *J*=3.5 Hz); 1.84 (bs, OH); 1.48 (t, 2H, *J*=3.5 Hz); 0.09 (s, 9H); ^{13}C NMR (100 MHz, CDCl$_3$) ppm: 84.7, 77.4, 51.9, 7.3, -1.9; TLC: 4:1 hexanes/EtOAc; R$_f$ ether: 0.9, stained red; R$_f$ alcohol: 0.4, stained red; *p*-anisaldehyde visualization; Elemental analysis calculated for C$_7$H$_{14}$OSi: C: 59.09, H: 9.92; Found: C: 59.03, H: 10.06

IV. Synthesis and Characterization of Copper(II) Paddlewheel Complexes

Possessing Fluorinated Carboxylate Ligands

1. Introduction

The use of ^{19}F NMR as a probe of protein structure and dynamics has been found in the scientific literature for quite some time, and a number of reviews have been devoted to this field of study.[62-64] There are many aspects of using fluorine-labeled proteins in such studies that make them quite attractive. For example, the fluorine atom is similar in size to the hydrogen atom, and even though it possesses a considerably different dipole moment, it is expected to impart little perturbation to the structure, stability, and function of the native protein.[65] Fluorine is not found in naturally occurring proteins, so any peaks observed in a ^{19}F NMR spectrum are certain to arise from the presence of the fluorine-labeled amino acids in the protein. In addition, the fluorine nucleus is extremely sensitive to its local chemical environment and to local shielding effects, resulting in well-resolved peaks in a one-dimensional NMR spectrum.[66] This sensitivity to local chemical environment enables ^{19}F NMR to probe protein structure on an amino acid residue level, an area where circular dichroism and fluorescence spectroscopy often fail.

Though there are numerous examples of proteins that have been characterized by ^{19}F NMR studies,[62,64] only a small number of these have investigated the nature of metal binding proteins. Previous reports of ^{19}F NMR being used to probe metal binding in proteins describe the use of fluorinated substrates to identify and quantify the allosteric states in insulin,[67] labeled proteins containing 4F-Phe or 3F-Tyr residues that are in close proximity to a metal binding center to detect conformational changes during ligation,[68,69]

or cysteine ligands that have been chemically modified with 4-(perfluoro-*tert*-butyl)-phenyliodoacetamide to detect the polymerization of actin.[70] However, there are no reports of the use of a fluorinated amino acid that coordinates directly to metal ions.

Given the dearth of ^{19}F NMR data for metalloprotein systems, it is prudent to use small molecule model systems to develop a better understanding of how the fluorine-19 nucleus will behave in the presence of metal ions. In this report, a model system comprised of copper(II) complexes possessing fluorinated carboxylate ligands was synthesized and characterized. This system was chosen because carboxylate residues (aspartate and/or glutamate) are known to directly bind metal ions in proteins and Cu(II) coordination sites are found in a variety of biological enzymes. Dysfunctional copper binding is also believed to play a part in the pathogenesis of Cruetzfeldt-Jacob disease.[71] In addition to playing an important physiological role, copper carboxylate complexes have been investigated for a variety of other applications, including catalytic chemical bond activation,[72] the preparation of metal oxide materials,[73] the supra-molecular assembly of metal ions,[74] and studying the fundamental nature of metal-metal interactions.[75]

Due to the paramagnetic nature of Cu(II), NMR spectra of complexes possessing the metal often exhibit extensive line broadening. As a result, ^{19}F NMR studies on paramagnetic copper coordination compounds are quite limited. Based on studies completed with H-BPMP (2,6-bis[(bis(2-pyridyl-methyl)amino)methyl]4-methylphenol) based[76] and perfluorocarboxylate[77] ligands, as the fluorine atom is further removed from the bound Cu(II) ion, the change in chemical shift should be less and the peaks should become less broadened. The effect of the paramagnetic copper is also thought to be

lessened if the fluorine nucleus is on a substituent with more rotational freedom and if there is no π conjugation on the ligand between the copper and fluorine atoms.[76,77]

The primary aim of this work was to compare the effect of paramagnetic copper(II) on fluorine nuclei located on tri-fluoroalkyl and mono-fluoroaryl carboxylates, and to determine the copper-fluorine distance that provides the optimum combination of minimal line broadening and chemical shift sensitivity in ^{19}F NMR. It was hypothesized that the trifluoropentanoate complex would be the most useful because it has the most removed fluorines. To this end, a series of fluorinated carboxylic acids were reacted with copper(II) hydroxide (Scheme 4.1). The composition of compounds **1-6** was verified by elemental analysis and a qualitative comparison of the ^{19}F NMR spectra carried out. The synthesis of this set of compounds also provided an opportunity to determine how subtle changes in the carboxylate ligand affected the solid state structural properties of the dimeric copper(II) paddlewheel complexes **1**, **2**, **4**, and **6**.

$$2Cu(OH)_2 + 4RCOOH \xrightarrow{\text{MeOH}}$$

$$\left[R-C\begin{array}{c} O-Cu \\ O-Cu \end{array} \right]_4$$

1: $R=o\text{-}C_6H_4F$
2: $R=m\text{-}C_6H_4F$
3: $R=p\text{-}C_6H_4F$
4: $R=CH_2CF_3$
5: $R=CH(CH_3)CF_3$
6: $R=(CH_2)_3CF_3$
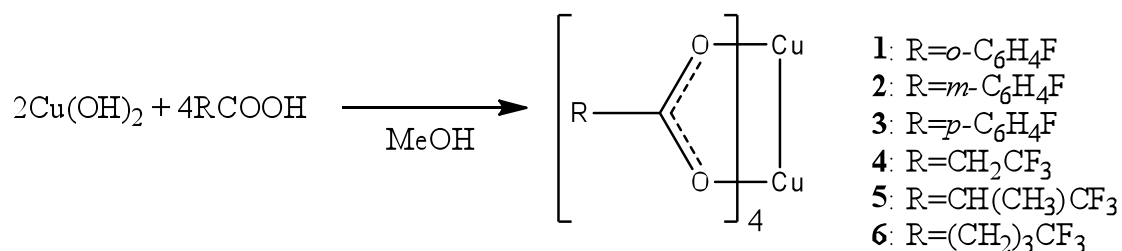
Scheme 4.1: Synthesis of paddlewheel-type copper carboxylates

2. Results and Discussion

2.1 Synthesis

Compounds **1-6** were synthesized by the straightforward reaction of the parent carboxylic acids with copper(II) hydroxide in alcoholic solvents. Upon reaction, the dark green reaction mixtures turned blue/blue-green and all of the subsequent solid carboxylate complexes, except for compound **3**, were recrystallized in good yields. After

being used in X-ray crystallographic studies, the crystals were dried *in vacuo* and used

for all subsequent analyses.

2.2 IR

      Compounds **1-6** exhibited a weakening of the C=O bond, due to the π

delocalization of the carboxylate functionality that occurred upon deprotonation of the

parent acid (Table 4.1). The fluorobenzoate copper complexes (**1-3**) underwent a similar

decrease in the C=O absorption (127-131 cm^{-1}), whereas the C=O stretch in the alkyl

chain analogues (**4-6**) was found to be dependent on the length of the carbon chain

[decrease in C=O stretch: **4**, 93 cm^{-1}; **5**, 119 cm^{-1}; **6**, 143 cm^{-1}; see Table 4.1). That the

placement of the fluorine on the phenyl ring had little effect on the IR properties of

compounds **1-3** is likely due to the π system's ability to similarly transmit the electronic

effects of the fluorine nucleus from any position on the ring. This is in agreement with

work done by Boiadjiev and Lightner, in which it was found that moving the fluorine to

different locations on the phenyl ring had much less effect on the pK_a of the benzoic acid

than did changing the distance between the carboxylic acid and the fluorine nucleus in the

alkyl chain derivatives.[78]

Compound	Parent Acid Absorption	Copper(II) Complex Absorption
1	1694	1565
2	1687	1556
3	1682	1555
4	1733	1640
5	1713	1594
6	1731	1588

Table 4.1: C=O stretch of compounds **1-6** and parent carboxylic acids (cm^{-1})

      Surprisingly, there is very little IR data for structurally analogous compounds

available in the literature. Data are available for two derivatives of a copper(II) dimer

possessing the trifluoroacetate ligand. The complex possessing a terminal THF solvent

ligand exhibited a C=O absorbance of 1684 cm^{-1}, whereas its isopropoxyethanol

congener displayed a C=O stretch at 1706 cm^{-1}.[73] These are both higher than the C=O

stretch found in **4**, and follow the trend of higher energy carbonyl absorptions being

associated with shorter fluorinated alkyl chains. It appears that as the fluorine atom is

farther removed from the carboxylate moiety, the C=O stretch is weakened, presumably

due to the fact that the carboxylate anion is not stabilized as much by the electron-

withdrawing effects of the more remote fluorine nuclei. By the fifth carbon, there

appears to be little effect on the IR absorption of the C=O. The non-fluorinated cousin of

compound **4**, $Cu_2(OOCCH_2CH_3)_4$, was reported to exhibit a C=O stretching frequency of

1628 cm^{-1}, slightly lower than that reported for compound **4**.[79] Again, this seems to

indicate that the presence of fluorine on the ligand helps stabilize the anion. The IR

absorptions of compound **5** and anhydrous copper(II) hexanoate[80] are nearly identical,

presumably due to the limited electron withdrawing ability of the fluorine nucleus at this

distance. No previous IR data could be found for either fluorinated or non-fluorinated

benzoate copper complexes in the dinuclear paddlewheel configuration.

2.3. ^{19}F NMR

When analyzed using fluorine-19 NMR, all six compounds showed some degree

of line broadening along with a change in chemical shift compared to the parent acid

(Table 4.2 and Figure 4.1). Compounds **1-3** showed no discernable pattern relating

chemical shift sensitivity or line broadening to the distance between the fluorine nucleus

and the copper ion. The change in chemical shifts between the free acid and benzoate

salts were -0.2, +3.1, and -2.8 ppm for **1**, **2**, and **3**, respectively. Complex **2** yielded the

greatest peak width at half-height (500 Hz), whereas compounds **1** (160 Hz) and **3** (175

Hz) displayed similar line broadening and were much narrower than **2** (Table 4.2). For

the alkyl analogues, the ^{19}F NMR resonance for compound **4**, underwent the largest

chemical shift compared to the free acid (12.6 ppm), as expected. The resonance for

compound **5** shifted 2.0 ppm, whereas compound **6** exhibited very little change in

chemical shift (-0.3 ppm, Table 4.2). The three-carbon propionate salt (**4**) displayed a

considerable amount of line broadening (600 Hz) compared to the four-carbon

methylbutyrate (**5**, 75 Hz) and five-carbon pentanoate (**6**, 35 Hz) salts (Figure 4.1). As

previously reported, the lack of π conjugation between the copper(II) ion and fluorine

nucleus, along with a larger distance between the copper metal center and fluorine

nucleus, results in less line broadening in the ^{19}F NMR spectrum.[76,77]

	Acid Peak (ppm)	Complex Peak (ppm)	Change (ppm)	Peak Width (Hz)
1	-111.6	-111.8	-0.2	160
2	-114.5	-111.4	+3.1	500
3	-108.1	-110.9	-2.8	175
4	-64.7	-52.1	+12.6	600
5	-74.7	-72.7	+2.0	75
6	-67.3	-67.6	-0.3	35

Table 4.2: Chemicals shifts and peak widths for compounds **1-6**
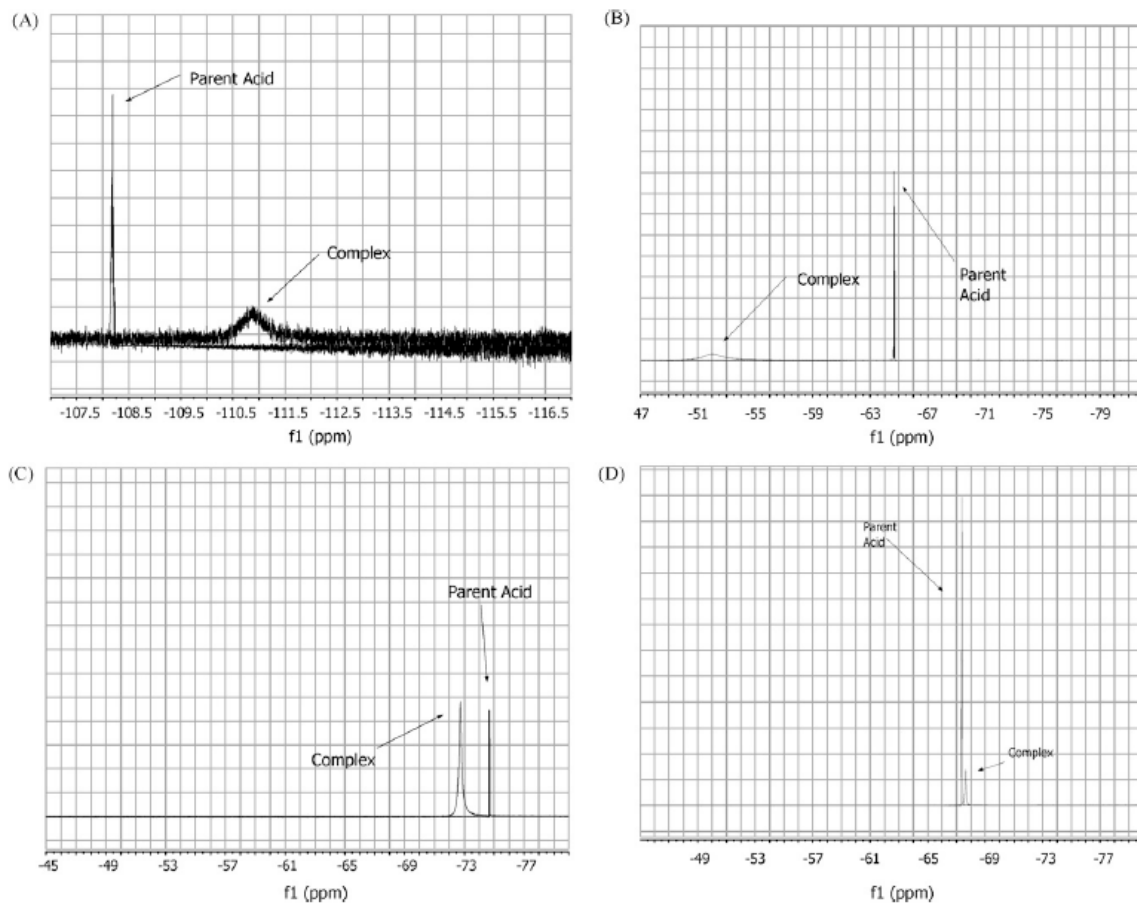
Figure 4.1: ^{19}F NMR spectra of **3**(A), **4**(B), **5**(C) and **6**(D)

Though no studies have looked at the effect of metals on the ^{19}F NMR spectra of fluorinated benzoates, Boiadjiev and Lightner found that the ^{19}F NMR chemical shift of o*rtho*- and *para*-fluorobenzoic acid are much more sensitive to deprotonation of the carboxylate than the *meta*- isomer, with the *para*-isomer being the most sensitive.[78] For our compounds, the *meta*- isomer (**2**) is the most sensitive to the presence of the copper atom, with a significantly larger change in chemical shift than the *ortho*- isomer (**1**). Previous ^{19}F NMR studies have been carried out on the perfluorinated analogues of compounds **4** and **6**, as well as a perfluorobutyrate copper complex that is similar to compound **5**.[77] However, given that these studies were done under significantly different experimental conditions, a conclusive comparison is not possible. It is noted that this

data seem to indicate that the use of the trifluoro carboxylate ligands in **4-6** may impart less line broadening and a greater range of chemical shift sensitivity as compared to perfluorinated carboxylates. As mentioned above, fluorine-19 NMR studies have been previously carried out on the parent carboxylic acids from compounds **1-5**.[78] Based on these data, it is apparent the chemical shift change upon forming the copper(II) complex is greater than the change observed during the simple deprotonation of the acid in both the alkyl and aryl derivatives.

The effect of the copper(II) ion dissipates rapidly as the length of the alkyl chain is lengthened. After adding a fifth carbon in the alkyl carboxylate , there is no significant effect on the chemical shift of fluorine. Therefore, the most useful compound for detecting the presence of copper ions seems to be **5**. Though it undergoes some increase in line broadening, it is much less than that observed for compound **4** (as well as compounds **1-3**), and it exhibits a more easily detectable change in chemical shift than in compound **6**.

2.4. Crystal Structures

The crystal structures obtained for **1, 2, 3**[81], **4,** and **6** indicate that the compounds exist in the dinuclear paddlewheel configuration that is common among copper(II) carboxylates. In general, these compounds consist of two copper(II) metal centers bridged by four carboxylate ligands. The distorted octahedral geometry is completed by a Cu-Cu interaction, and by solvent ligands bound at the axial position (**1-4**) or by carboxylate oxygens from an adjoining copper dimer (**6**).

Compounds **1, 2,** and **3** are isostructural (Figure 4.2, a derivative of compound **3**, possessing ethanol ligands in the axial position, has been previously characterized by X-

ray crystallography[81]). The Cu-Cu distances of 2.5882(13), 2.614(2), and 2.5843(8) Å, respectively, are in general agreement with the previously reported 2,6-difluorobenzoate analogue [Cu-Cu distance: 2.6139(2) Å $(Cu_2(OOCC_6H_4F_2)_4(H_2O)_2)$].[82] The Cu-$O_{carboxy}$ distances for **1-3,** ranging from 1.926(7)-1.966(8) Å, are also in agreement with the 2,6-difluorobenzoate copper(II) structure (average Cu-$O_{carboxy}$ = 1.9655(7) Å)[82], and as expected, are found to be shorter than the Cu-O_{solv} distances (**1**: 2.126(3) Å; **2**: average = 2.142(7) Å; **3**: 2.141(2) Å[83]). Karipides and White report that the copper(II) 2,6-difluorobenzoate species[84] has a C-F···H-O_{water} distance of 2.962 Å, which they describe as the shortest known organic hydrogen bond of its kind. Lim *et al.* found the same compound showed a C-F···H-O_{water} distance of 2.928 Å.[82] Compound **1** shows a C-F···H-O_{MeOH} bond length of 2.955 Å, intermediate of these two previous distances. In addition to this particular interaction, other hydrogen bonds can be found in compounds **1** and **2**. Unbound methanol molecules reside in the spaces between the paddle wheels and are held in place by hydrogen bonds with the fluorine and carboxylate oxygens. The hydrogen bonds cause some distortion in the paddlewheel, though neither **1** nor **2** have $O_{carboxy}$-Cu-$O_{carboxy}$ angles that vary more than 8° from a right angle.
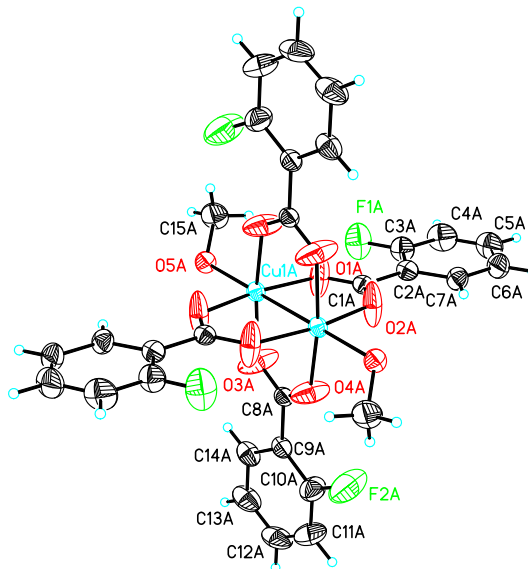
Figure 4.2: Crystal Structure of **1** showing paddlewheel configuration with solvent coordination.

The crystal structures of **4** and **6** also exist in the standard dinuclear paddlewheel configuration (Figures 4.3 and 4.4). Compound **4** possesses axial water ligands, whereas compound **6** has no terminal ligand, and therefore forms a tetramer where carboxylate oxygens of neighboring dimers ($O_{carboxy'}$) complete the copper coordination sphere. As found for all analogous paddlewheel complexes, the Cu-$O_{carboxy}$ distances for **4** and **6** (1.9534(1)-1.999(3) Å) are shorter than the Cu-O_{H20} (**4**: 2.1088(1)-2.1440(11) Å) and Cu-$O_{carboxy'}$ (**6**: 2.201(3)-2.205(3) Å) distances. Two previously published structures of the non-fluorinated propionate complex, $[Cu_2(OOCCH_2CH_3)]$,[79,85] are structurally analogous to compound **4**. However, the Cu-Cu distance seen in **4** (2.614(2) Å) is slightly longer than that of its non-fluorinated analogues (2.5826(12) and 2.578(4) Å). There are no previously reported structural congeners for compound **6**; however comparison to compound **4** indicates that the Cu-Cu distance for **6** (2.580 Å) is slightly shorter. This can be attributed to the previously reported observation that as the electron withdrawing

ability of the carboxylate ligand increases, the Cu-Cu interatomic distance also increases.[73,83]
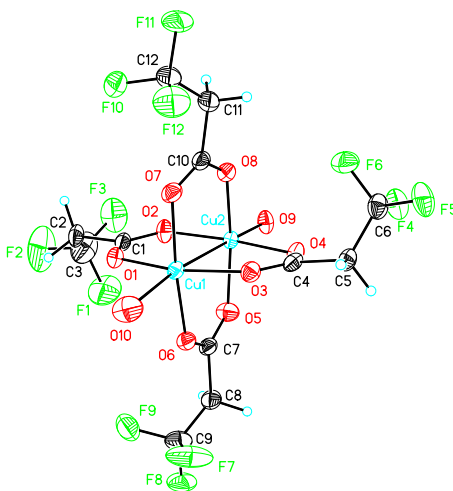
Figure 4.3: Crystal Structure of **4** showing paddlewheel configuration with solvent oxgyens coordinating in the apical position.
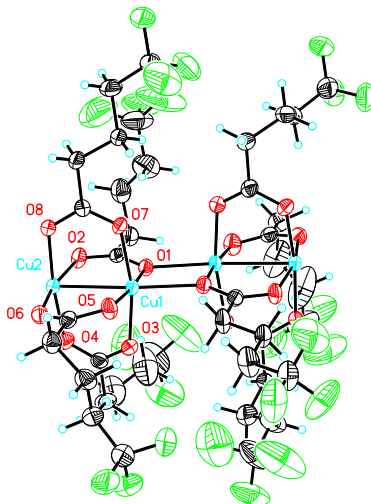
Figure 4.4: Crystal Structure of **6** showing double paddlewheel configuration with no solvent coordination.

Compound **6** lacks axial solvent ligands and exists as a tetramer, which is unique among the structures reported here. A similar copper tetramer was previously prepared using a hexanoate ligand system, though it is noted this complex possessed terminal urea ligands.[86] That hexanoate complex (Cu-Cu: 2.5791(5) Å, Cu-$O_{carboxy}$: 1.94-1.96 Å; Cu-$O_{carboxy'}$: 2.01 Å) is comparable in metal center structure to **6** (Cu-Cu, 2.580 Å; Cu-

$O_{carboxy}$, 1.932(3)-1.999(3) Å; Cu-$O_{carboxy'}$, 2.201(3)-2.205(3) Å). Upon inspection of the extended crystal network of compound **6**, it was found that the tetrameric units polymerized via bridging carboxylate oxygens ($O_{carboxy'}$), analogous to the formation of the tetramer (Figure 4-5). This gives rise to a chain of Cu···Cu-Cu···Cu interactions, which alternate between 2.57919(5) and 3.210 Å. These distances are in agreement with previously reported polymeric structures with carboxylate ligands including methylbutyrate[87] (Cu-Cu: 2.5893 Å, Cu···Cu 3.268 Å), hexanoate[85] (Cu-Cu: 2.579 Å, Cu···Cu 3.236 Å), heptanoate[88] (Cu-Cu: 2.578 Å, Cu···Cu 3.232 Å), octanoate[89] (Cu-Cu: 2.575 Å, Cu···Cu 3.269 Å), and decanoate[90] (Cu-Cu: 2.624 Å, Cu···Cu 3.365 Å). Though other polymeric copper(II) carboxylates have been reported,[74,75,85,87-90] compound **6** appears to be the first such structure possessing a fluorinated carboxylate ligand and subsequent close C-F···H-C interactions between individual polymer chains (C-F···H-C distances of 2.448, 2.823, and 3.044 Å).
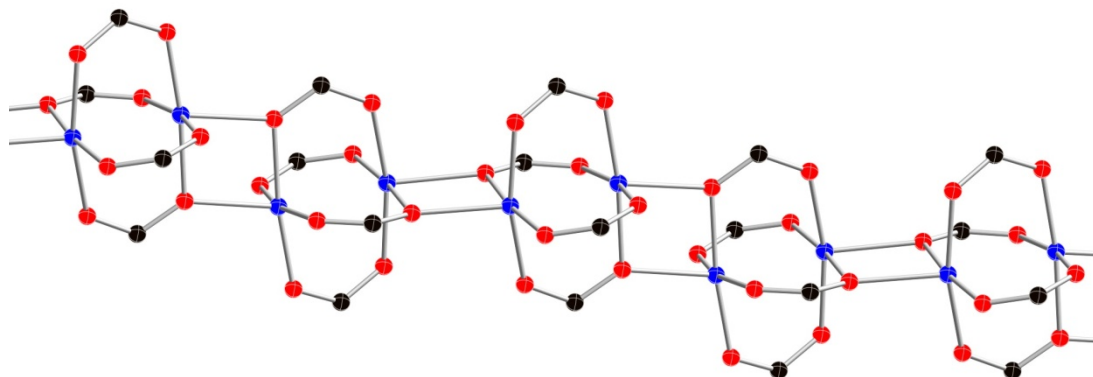
Figure 4.5: Macromolecular structure of **6** showing direct coordination between Cu and O of adjacent paddlewheels (copper atoms shown in blue, oxygen shown in red, carbon shown in black; carbons beyond C1 omitted).

3. Conclusion

The synthesis and characterization of the series of monofluorobenzoate and trifluoroalkyl carboxylate copper(II) complexes, **1-6**, reveals that the 3-(trifluoromethyl)butyrate species [$Cu_2(OOCCH(CF_3)CH_3)_4$; **5**] provides the optimal combination of reduced line broadening and chemical shift sensitivity in ^{19}F NMR studies. This is in contrast to our expectation of the pentanoate salt being most useful: it experienced only a minimal change in chemical shift. This result suggests that **5** represents a potential structural model for developing fluorinated probes that could be used in ^{19}F NMR studies of copper(II) binding proteins because the lower degree of line broadening reduces the uncertainly in assigning the chemical shift to a peak in studying conformational changes in proteins. In addition, results from X-ray crystallography experiments indicate that the use of trifluoroalkyl carboxylate ligands allow for the straightforward tuning of metal-metal interatomic distances in transition metal carboxylate paddlewheel complexes. Given the fact that compound **6** affords an extended network of copper(II)-copper(II) interactions, the trifluoropentanoate ligand may provide an opportunity to develop analogous supramolecular networks with other metals.

4. Experimental

4.1. General Procedures

2-, 3-, and 4-fluorobenzoic acids and were purchased from Sigma-Aldrich; 3,3,3-trifluoropropionic acid, 3-(trifluoromethyl)butyric acid, and 5,5,5-trifluoropentanoic acid were purchased from Oakwood Products, Inc; and $Cu(OH)_2$ was purchased from Alfa Aesar. All reagents were used without further purification.

IR data were obtained on a Perkin Elmer FT-IR Paragon 500 using a KBr pellet. ^{19}F NMR were obtained on a Varian Inova 400 spectrometer at 376 MHz. All samples were dissolved in a CD_3OD with 0.08% (v/v) C_6F_6. Data are reported as chemical shifts (ppm) relative to C_6F_6. Peak width at half-height was estimated using Mestre-C (v. 4.9.9.0).[91]

For X-ray crystallography, suitable crystals of **1**, **2**, **4**, and **6** were coated with Paratone N oil, suspended in a small fiber loop and placed in a cooled nitrogen gas stream at 173 K on a Bruker D8 APEX II CCD sealed tube diffractometer with graphite monochromated Cu K$_\alpha$ (1.54178 Å) radiation. Data were measured using a series of combinations of phi and omega scans with 10 s frame exposures and $0.5°$ frame widths. Data collection, indexing and initial cell refinements were all carried out using APEX II software.[22] Frame integration and final cell refinements were done using SAINT software.[23] The structure was solved using direct methods and difference Fourier techniques (SHELXTL, V6.12).[24] Hydrogen atoms were placed their expected chemical positions using the HFIX command and were included in the final cycles of least squares with isotropic U_{ij} 's related to the atom's ridden upon. All non-hydrogen atoms were refined anisotropically. Scattering factors and anomalous dispersion corrections are taken from the *International Tables for X-ray Crystallography*.[25] Structure solution, refinement, graphics and generation of publication materials were performed by using SHELXTL, V6.12 software.

4.1.1. General procedure for synthesis of copper(II) aryl carboxylate salts

The fluorinated acid (**1**: 504 mg, 3.6 mmol; **2**: 559 mg, 4.0 mmol; **3**: 490 mg, 3.5 mmol) was dissolved in methanol, and to the solution was added $MgSO_4$ (1 g) and excess

$Cu(OH)_2$ (**1**: 515 mg, 5.2 mmol; **2**: 527 mg, 5.4 mmol; **3**: 488 mg, 5.0 mmol). The

suspensions were stirred for 20 minutes, when which a blue or blue/green color was

noticeable. The solid, consisting of $MgSO_4$ and excess $Cu(OH)_2$, was filtered off and the

solvent reduced *in vacuo*. Crystals of compounds **1-3** were then grown at low

temperature (5-ˉ20º C), isolated, and used for all subsequent analyses.

4.1.2. General procedure for synthesis of copper(II) alkyl carboxylate salts

The fluorinated acid (**4**: 695 mg, 4.4 mmol; **5**: 515 mg, 4.0 mmol; **6**: 526 mg, 3.3

mmol) was reacted with ≤ 0.5 equivalents of $Cu(OH)_2$ (**4**: 159 mg, 1.6 mmol; **5**: 193 mg,

1.9 mmol; **6**: 156 mg, 1.5 mmol). The starting materials were dissolved separately in

ethanol, the solutions were combined, and the reaction mixture was refluxed for 3 hours.

As the reflux progressed, the solutions turned blue or blue/green. The solvent was then

removed by rotary evaporation to yield the solid product, which was dried under vacuum

and moderate heat (~0.5 torr, 50° C). Crystals were obtained by slow evaporation from

methanol, isolated, and used for all subsequent analyses. (Synthesis by Rebekah

Cordeiro, Crystallization and Characterization by A. N. W.)

4.2. Characterization data for compounds **1-6**

4.2.1. Bis[(2-fluorobenzoate])copper(II) (**1**)

76.5% yield (by recrystallization at 5°C); blue-green needles; IR (KBr pellet),

cm^{-1}: 1615 (aromatic C-C), 1565 (C=O), 1406 (C-F); ^{19}F NMR (376 MHz) ppm: -111.8

(s); Elemental Analysis, calculated for $CuC_{14}H_8O_4F_2$: C: 49.18, H: 2.36; Found: C: 48.75,

H: 2.31.

4.2.2. Bis[(3-fluorobenzoate)]copper(II) (**2**)

54.2% yield (by recrystallization at -20°C); blue-green prisms; IR (KBr pellet),

cm^{-1}: 1595 (aromatic C-C), 1556 (C=O), 1415 (C-F); ^{19}F NMR (376 MHz, CD$_3$OD) ppm:

-111.4 (s); Elemental Analysis, calculated for CuC$_{14}$H$_8$O$_4$F$_2$•0.5H$_2$0: C: 47.92, H: 2.59;

Found: C 47.83: H: 2.30.

4.2.3. Bis[(4-fluorobenzoate)]copper(II) (**3**)

5% yield (by recrystallization at 0°C); small blue-green crystals, rapidly degraded

to a light blue solid when exposed to air; IR (KBr), cm^{-1}: 1607 (aromatic C-C), 1555

(C=O), 1421 (C-F); ^{19}F NMR (376 MHz, CD$_3$OD) ppm: ⁻110.9 (s); Elemental Analysis,

calculated for CuC$_{14}$H$_8$O$_4$F$_2$: C: 49.2, H: 2.3 Found: C:47.2, H: 2.3.

4.2.4. Bis[(3,3,3-trifluoropropionate)]copper(II) (**4**)

88.7% yield; green-blue powder; IR (KBr), cm^{-1}: 1640 (C=O), 1466 (C-F); ^{19}F

NMR (376 MHz, CD$_3$OD) (ppm): -52.1 (s); Elemental Analysis, calculated for

CuC$_6$H$_4$O$_4$F$_6$: C: 22.67, H:1.27; Found: C 22.68, H: 1.20.

4.2.5. Bis[(3-(trifluoromethyl)butyrate)]copper(II) (**5**)

52.2% yield; blue powder; IR (KBr) cm^{-1}: 1594 (C=O), 1431 (C-F); ^{19}F NMR

(376 MHz, CD$_3$OD) ppm: -72.7 (s); Elemental Analysis, calculated for CuC$_{10}$H$_{10}$O$_4$F$_6$: C:

32.29, H: 2.71; Found: C: 31.98, H: 3.16.

4.2.6. Bis[(5,5,5-trifluoropentanoate)]copper(II) (**6**)

34.7% yield; blue powder; IR (KBr) cm^{-1}: 1588 (C=O), 1424 (C-F); ^{19}F NMR

(376 MHz, CD$_3$OD) ppm: -67.6 (s); Elemental Analysis, calculated for CuC$_{10}$H$_{12}$O$_4$F$_6$: C:

32.12, H: 3.24; Found: C: 32.36, H: 3.22.

5. Notes

Crystallographic data (excluding structure factors) for the structures in this paper

have been deposited with the Cambridge Crystallographic Data Centre as supplementary

publication nos. CCDC 703384 (compound **1**), 703385 (compound **2**), 703386

(compound **4**), and 703383 (compound **6**). Copies of the data can be obtained, free of charge, on application to CCDC, 12 Union Road, Cambridge CB2 1EZ, UK (fax: +44 1223 336033 or e-mail: deposit@ccdc.cam.ac.uk)

V. References

(1)   Heron, M.; Tejada-Vera, B. *National Vital Statistics Reports* **2009**, *58*.

(2)   Kostova, I. *Recent Patents on Anti-Cancer Drug Discovery* **2006**, *1*, 1.

(3)   Kostova, I. *Anti-Cancer Agents Med. Chem.* **2006**, *6*, 19.

(4)   Hudson, Z. D.; Sanghvi, C. D.; Rhine, M. A.; Ng, J. J.; Bunge, S. D.; Hardcastle, K. I.; Saadein, M. R.; MacBeth, C. E.; Eichler, J. F. *Dalton Trans.* **2009**, 7473.

(5)   Marcon, G.; Carotti, S.; Coronnello, M.; Messori, L.; Mini, E.; Orioli, P.; Mazzei, T.; Cinellu, M. A.; Minghetti, G. *J. Med. Chem* **2002**, *45*, 1672.

(6)   McCann, M.; Coyle, B.; McKay, S.; McCormack, P.; Kavanagh, K.; Devereux, M.; McKee, V.; Kinsella, P.; O'Connor, R.; Clynes, M. *BioMetals* **2004**, *17*, 635.

(7)   Palanichamy, K.; Ontko, A. C. *Inorg. Chim. Acta* **2006**, *359*, 44.

(8)   Shaw, C. F. *Chem. Rev.* **1999**, *99*, 2589.

(9)   Sun, R. W.; Li, C. K.; Ma, D.; Yan, J. J.; Lok, C.; Leung, C.; Zhu, N.; Che, C. *Chem. Eur. J.* **2010**, *16*, 3097.

(10)   Thang, D. C.; Jacquignon, P.; Dufour, M. *J. Heterocycl. Chem.* **1976**, *13*, 641.

(11)   Tiekink, E. R. T. *Crit. Rev. Oncol. Hematol.* **2002**, *42*, 225.

(12)   Wong, E.; Giandomenico, C. M. *Chem. Rev.* **1999**, *99*, 2451.

(13)   Zhang, C. X.; Lippard, S. J. *Curr. Opin. Chem. Biol.* **2003**, *7*, 481.

(14)   Casini, A.; Cinellu, M. A.; Minghetti, G.; Gabbiani, C.; Coronnello, M.; Mini, E.; Messori, L. *J. Med. Chem* **2006**, *49*, 5524.

(15)   Messori, L.; Orioli, P.; Tempi, C.; Marcon, G. *Biochem. Biophys. Res. Commun.* **2001**, *281*, 352.

(16)   Coronnello, M.; Marcon, G.; Carotti, S.; Caciagli, B.; Mini, E.; Mazzei, T.; Orioli, P.; Messori, L. *Oncol. Res.* **2001**, *12*, 361.

(17)   Chew, E.-H.; Lu, J.; Bradshaw, T. D.; Holmgren, A. *FASEB J.* **2008**, *22*, 2072.

(18)   Verhoeven, J. W.; Van Der, T. E. B.; Steemers, F. J.; Verboom, W.; Reinhoudt, D. N.; Hofstraat, J. W.; Koninklijke Philips Electronics N.V.: 2008.

(19)   Abbate, F.; Orioli, P.; Bruni, B.; Marcon, G.; Messori, L. *Inorganica Chimica Acta* **2000**, *311*, 1.

(20)   Pia Rigobello, M.; Messori, L.; Marcon, G.; Agostina Cinellu, M.; Bragadin, M.; Folda, A.; Scutari, G.; Bindoli, A. *J. Inorg. Biochem.* **2004**, *98*, 1634.

(21)   Rhine, M., Honors Thesis, Emory University, 2009.

(22)   APEX; II ed.; Bruker AXS, Inc.: Madison, WI, 2005.

(23)   SAINT; 6.45A ed.; Bruker AXS, Inc.: Madison, WI, 2003.

(24)   SHELXTL; 6.12 ed.; Bruker AXS, Inc: Madison, WI, 2002.

(25)   *International Tables for X-ray Crystallography*; Wilson, A. J. C., Ed.; Kynoch Academic: Dordrect, 1992; Vol. C.

(26)   Arnér, E. S. J.; Sarioglu, H.; Lottspeich, F.; Holmgren, A.; Böck, A. *J. Mol. Bio.* **1999**, *292*, 1003.

(27)   Skehan, P.; Storeng, R.; Scudiero, D.; Monks, A.; McMahon, J.; Vistica, D.; Warren, J. T.; Bokesch, H.; Kenney, S.; Boyd, M. R. *J. Natl. Cancer Inst.* **1990**, *82*, 1107.

(28)   Kent, K.; Clubbs, E.; Harper, W.; Bomser, J. *Lipids* **2008**, *43*, 143.

(29)   Nava, V. E.; Cuvillier, O.; Edsall, L. C.; Kimura, K.; Milstien, S.; Gelmann, E. P.; Spiegel, S. *Cancer Res.* **2000**, *60*, 4468.

(30)   Padrón, J. M. *Curr. Med. Chem.* **2006**, *13*, 755.

(31)   Menaldino, D. S.; Bushnev, A.; Sun, A.; Liotta, D. C.; Symolon, H.; Desai, K.; Dillehay, D. L.; Peng, Q.; Wang, E.; Allegood, J.; Trotman-Pruett, S.; Sullards, M. C.; Merrill, A. H. *Pharmacol. Res.* **2003**, *47*, 373.

(32)   Maurer, B. J.; Melton, L.; Billups, C.; Cabot, M. C.; Reynolds, C. P. *J. Natl. Cancer Inst.* **2000**, *92*, 1897.

(33)   Sakakura, C.; Sweeney, E. A.; Shirahama, T.; Hakomori, S.-i.; Igarashi, Y. *FEBS Lett.* **1996**, *379*, 177.

(34)   Pchejetski, D.; Golzio, M.; Bonhoure, E.; Calvet, C.; Doumerc, N.; Garcia, V.; Mazerolles, C.; Rischmann, P.; Teissie, J.; Malavaud, B.; Cuvillier, O. *Cancer Res.* **2005**, *65*, 11667.

(35)   Schwartz, G. K.; Ward, D.; Saltz, L.; Casper, E. S.; Spiess, T.; Mullen, E.; Woodworth, J.; Venuti, R.; Zervos, P.; Storniolo, A. M.; Kelsen, D. P. *Clin. Cancer Res.* **1997**, *3*, 537.

(36)   Sánchez, A. M.; Malagarie-Cazenave, S.; Olea, N.; Vara, D.; Cuevas, C.; Díaz-Laviada, I. *Eur. J. Pharmacol.* **2008**, *584*, 237.

(37)   Cuadros, R.; Montejo de Garcini, E.; Wandosell, F.; Faircloth, G.; Fernández-Sousa, J. M.; Avila, J. *Cancer Lett.* **2000**, *152*, 23.

(38)   Kossuga, M. H.; MacMillan, J. B.; Rogers, E. W.; Molinski, T. F.; Nascimento, G. G. F.; Rocha, R. M.; Berlinck, R. G. S. *J. Nat. Prod.* **2004**, *67*, 1879.

(39)   Clark, R. J.; Garson, M. J.; Hooper, J. N. A. *J. Nat. Prod.* **2001**, *64*, 1568.

(40)   Jares-Erijman, E. A.; Bapat, C. P.; Lithgow-Bertelloni, A.; Rinehart, K. L.; Sakai, R. *J. Org. Chem.* **1993**, *58*, 5732.

(41)   Garrido, L.; Zubía, E.; Ortega, M. J.; Naranjo, S.; Salvá, J. *Tetrahedron* **2001**, *57*, 4579.

(42)   Humpf, H.-U.; Schmelz, E.-M.; Meredith, F. I.; Vesper, H.; Vales, T. R.; Wang, E.; Menaldino, D. S.; Liotta, D. C.; Merrill, A. H. *J. Biol. Chem.* **1998**, *273*, 19060.

(43)   Molinski, T. F.; Makarieva, T. N.; Stonik, V. A. *Angew. Chem. Int. Ed.* **2000**, *39*, 4076.

(44)   Kong, F.; Faulkner, D. J. *J. Org. Chem.* **1993**, *58*, 970.

(45)   Aiello, A.; Fattorusso, E.; Giordano, A.; Menna, M.; Navarrete, C.; Muñoz, E. *Bioorg. Med. Chem.* **2007**, *15*, 2920.

(46)   Gulavita, N. K.; Scheuer, P. J. *J. Org. Chem.* **1989**, *54*, 366.

(47)   Jiménez, C.; Crews, P. *J. Nat. Prod.* **1990**, *53*, 978.

(48)   Katsuki, T.; Sharpless, K. B. *J. Am. Chem. Soc.* **1980**, *102*, 5974.

(49)   Caron, M.; Sharpless, K. B. *J. Org. Chem.* **1985**, *50*, 1557.

(50)   Sonogashira, K.; Tohda, Y.; Hagihara, N. *Tetrahedron Lett.* **1975**, *16*, 4467.

(51)   Kouanda, A., Honors Thesis, Emory University, 2010.

(52)   Balduzzi, S.; Brook, M. A.; McGlinchey, M. J. *Organometallics* **2005**, *24*, 2617.

(53)   Mastalerz, H. *J. Org. Chem.* **1984**, *49*, 4092.

(54)   Nativi, C.; Taddei, M.; Mann, A. *Tetrahedron Lett.* **1987**, *28*, 347.

(55)   Jervis, P. J.; Kariuki, B. M.; Cox, L. R. *Org. Lett.* **2006**, *8*, 4649.

(56)   Jervis, P. J.; Kariuki, B. M.; Cox, L. R. *Tetrahedron Lett.* **2008**, *49*, 2514.

(57)   Klaver, W. J.; Hiemstra, H.; Speckamp, W. N. *Tetrahedron* **1988**, *44*, 6729.

(58)   Majetich, G.; Lowery, D.; Khetani, V. *Tetrahedron Lett.* **1990**, *31*, 51.

(59)   Klaver, W. J.; Moolenaar, M. J.; Hiemstra, H.; Speckamp, W. N. *Tetrahedron* **1988**, *44*, 3805.

(60)   Pornet, J.; Damour, D.; Miginiac, L. *J. Organomet. Chem.* **1987**, *319*, 333.

(61)   Tong, R.; Valentine, J. C.; McDonald, F. E.; Cao, R.; Fang, X.; Hardcastle, K. I. *J. Am. Chem. Soc.* **2007**, *129*, 1050.

(62)   Gerig, J. T. *Prog. Nucl. Magn. Reson. Spectrosc.* **1994**, *26*, 293.

(63)   Gerig, J. T. In *Methods Enzymol.*; Norman, J. O., Thomas, L. J., Eds.; Academic Press: 1989; Vol. Volume 177, p 3.

(64)   Danielson, M. A.; Falke, J. J. *Annu. Rev. Biophys. Biomol. Struct.* **2003**, *25*, 163.

(65)   Frieden, C.; Hoeltzli, S. D.; Bann, J. G. In *Methods Enzymol.*; Jo M. Holt, M. L. J., Gary, K. A., Eds.; Academic Press: 2004; Vol. Volume 380, p 400.

(66)   Lau, E. Y.; Gerig, J. T. *Biophys. J.* **1997**, *73*, 1579.

(67)   Bonaccio, M.; Ghaderi, N.; Borchardt, D.; Dunn, M. F. *Biochemistry* **2005**, *44*, 7656.

(68)   Drake, S. K.; Bourret, R. B.; Luck, L. A.; Simon, M. I.; Falke, J. J. *J. Biol. Chem.* **1993**, *268*, 13081.

(69)   Dupureur, C. M.; Hallman, L. M. *Eur. J. Biochem.* **1999**, *261*, 261.

(70)   Heintz, D.; Kany, H.; Kalbitzer, H. R. *Biochemistry* **1996**, *35*, 12686.

(71)   Garnett, A. P.; Jones, C. E.; Viles, J. H. *Dalton Trans.* **2006**, 509.

(72)   Dikarev, E. V.; Andreini, K. W.; Petrukhina, M. A. *Inorg. Chem.* **2004**, *43*, 3219.

(73)   Zhang, J.; Hubert-Pfalzgraf, L. G.; Luneau, D. *Polyhedron* **2005**, *24*, 1185.

(74)   Aakeroy, C. B.; Schultheiss, N.; Desper, J. *Dalton Trans.* **2006**, 1627.

(75)   Li, S.; Mak, T. *Struct. Chem.* **1997**, *8*, 49.

(76)   Belle, C.; Beguin, C.; Gautier-Luneau, I.; Hamman, S.; Philouze, C.; Pierre, J. L.; Thomas, F.; Torelli, S.; Saint-Aman, E.; Bonin, M. *Inorg. Chem.* **2002**, *41*, 479.

(77)   Sobolev, A.; Krupoder, S.; Liskovskaya, T.; Danilovich, V. *J. Struct. Chem.* **2000**, *41*, 338.

(78)   Boiadjiev, S. E.; Lightner, D. A. *J. Phys. Org. Chem* **1999**, *12*, 751.

(79)   Chung, Y. H.; Wei, H. H.; Liu, Y. H.; Lee, G. H.; Wang, Y. *Polyhedron* **1998**, *17*, 449.

(80)   Doyle, A.; Felcman, J.; Gambardella, M. T. d. P.; Verani, C. N.; Tristão, M. L. B. *Polyhedron* **2000**, *19*, 2621.

(81)   Hu, R.-Z.; Liu, Z.-D.; Tan, M.-Y.; Zhu, H.-L. *Acta Crystallogr., Sect. E: Struct. Rep. Online* **2004**, *60*, m946.

(82)   Lim, E. K.; Teoh, S. G.; Teh, J. B.-J.; Fun, H.-K.; Yuen, C. W. *Acta Crystallogr., Sect. E: Struct. Rep. Online* **2007**, *63*, m991.

(83)   Cotton, F. A.; Dikarev, E. V.; Petrukhina, M. A. *Inorg. Chem.* **2000**, *39*, 6072.

(84)   Karipides, A.; White, C. *Acta Crystallogr., Sect. C: Cryst. Struct. Commun.* **1993**, *49*, 1920.

(85)   Simonov, Y.; Malinokskii, T. I. *Soviet Physics: Crystallography* **1970**, *15*, 310.

(86)   Kozlevcar, B.; Leban, I.; Petric, M.; Petricek, S.; Roubeau, O.; Reedijk, J.; Segedin, P. *Inorg. Chim. Acta* **2004**, *357*, 4220.

(87)   Campbell, G. C.; Reibenspies, J. H.; Haw, J. F. *Inorg. Chem.* **1991**, *30*, 171.

(88)   Ghermani, N. E.; Lecomte, C.; Rapin, C.; Steinmetz, P.; Steinmetz, J.; Malaman, B. *Acta Crystallogr., Sect. B: Struct. Sci* **1994**, *50*, 157.

(89)   Lomer, T. R.; Perera, K. *Acta Crystallogr., Sect. B: Struct. Sci* **1974**, *30*, 2913.

(90)   Lomer, T. R.; Perera, K. *Acta Crystallogr., Sect. B: Struct. Sci* **1974**, *30*, 2912.

(91)   Mestrec; 4.9.9.0 ed.; Mestrelab Research, SL: Santiago de Compostela, Spain.